Conformationally flexible core-bearing detergents with a hydrophobic or hydrophilic pendant: Effect of pendant polarity on detergent conformation and membrane protein stability

Aiman Sadaf,[a] Seonghoon Kim,[b] Hyoung Eun Bae,[a] Haoqing Wang,[c] Andreas Nygaard,[d] Yuki Uegaki,[e] Yang Du,[c,#] Chastine F. Munk,[d] Satoshi Katsube,[e] Jungnam Bae,[h] Chul Won Choi,[h] Hee-Jung Choi,[h] Bernadette Byrne,[g] Samuel H. Gellman,[f] Lan Guan,[e] Claus J. Loland,[d] Brian K. Kobilka,[c] Wonpil Im,[b] and Pil Seok Chae*[a]

[a] Department of Bionanotechnology, Hanyang University, Ansan 155-88 (KR) [b] Department of Biological Sciences, Chemistry, and Bioengineering, Lehigh University, Bethlehem, PA 18015 (USA) [c] Department of Molecular and Cellular Physiology, Stanford University, California 94305 (USA) [d] Department of Neuroscience, University of Copenhagen, Copenhagen, DK-2200 (Denmark) [e] Department of Cell Physiology and Molecular Biophysics, Center for Membrane Protein Research, School of Medicine, Texas Tech University Health Sciences Center, Lubbock, TX 79430 (USA) [f] Department of Chemistry, University of Wisconsin, Madison, Wisconsin 53706 (USA) [g] Department of Life Sciences, Imperial College London, London, SW7 2AZ (UK) [h] Department of Biological Sciences, Seoul National University, Seoul 08826 (KR)

E-mail address: pchae@hanyang.ac.kr

Abstract:

Membrane protein structures provide atomic level insight into essential biochemical processes and facilitate protein structure-based drug design. However, the inherent instability of these bio-macromolecules outside lipid bilayers hampers their structural and functional study. Detergent micelles can be used to solubilize and stabilize these membrane-inserted proteins in aqueous solution, thereby enabling their downstream characterizations. Membrane proteins encapsulated in detergent micelles tend to denature and aggregate over time, highlighting the need for development of new amphiphiles effective for protein solubility and stability. In this work, we present newly-designed maltoside detergents containing a pendant chain attached to a glycerol-decorated tris(hydroxylmethyl)methane (THM) core, designated GTMs. One set of the GTMs has a hydrophobic pendant (ethyl chain; E-GTMs), and the other set has a hydrophilic pendant (methoxyethoxylmethyl chain; M-GTMs) placed in the hydrophobic-hydrophilic interfaces. The two sets of GTMs displayed profoundly different behaviors in terms of detergent self-assembly and protein stabilization efficacy. These behaviors mainly arise from the polarity difference between two pendants (ethyl and methoxyethoxylmethyl chains) that results in a large variation in detergent conformation between these sets of GTMs in aqueous media. The resulting high hydrophobic density in the detergent micelle interior is likely responsible for enhanced efficacy of the M-GTMs for protein stabilization compared to the E-GTMs and a gold standard detergent DDM. A representative GTM, M-GTM-O12, was more effective for protein stability than some recently developed detergents including LMNG. This is the

first case study investigating the effect of pendant polarity on detergent geometry that correlates with detergent efficacy for protein stabilization.

Key words: *pendant polarity, detergent conformation, membrane proteins, protein stabilization, amphiphile design*

1. Introduction

Membrane proteins in cell membranes are key structural and functional components of all living organisms. Encoded by 20-30% of the open reading frames in the genomes of all living organisms, these bio-macromolecules are fundamental to cell physiology and play crucial roles in signal reception and transduction, inter-cellular communication, energy interconversion and material transport [1,2]. High-risk health disorders such as Alzheimer, cancer, and heart disease arise from dysfunction of membrane proteins[3] and therefore are key targets of currently marketed pharmaceutical agents [3,4]. The available structural information for these biopolymers has significantly increased our comprehension of various bio-cellular activities at a molecular level and is of prime importance for future protein structure-based drug design [5]. However, membrane proteins constitute only ~3% of the structural information available in the PDB [6]. The limited structural information is mainly due to the poor solubility and/or instability of membrane proteins in aqueous solution that needs to be managed effectively for downstream bio-physical characterizations. As they reside in lipid bilayers, membrane proteins comprise a membrane-embedded hydrophobic domain, flanked by the hydrophilic domains directly in contact with the water-based environment on either side of the membrane. The amphiphilic nature of membrane proteins renders them difficult to extract into aqueous solution and hence challenging to structurally and functionally characterize. Since the first successful crystallization of protein-detergent complex in 1985, use of detergent micelles as protein stabilizers has been a common practice for membrane protein structural study [7]. Like phospholipid molecules, detergent molecules are amphiphilic, comprising a hydrophilic head and hydrophobic tail groups, but, due to the different molecular geometry, detergents tend to form small micelles with a

globular or elliptical shape rather than planar bilayers. Detergent micelles are efficient at both degrading the membrane architecture and effectively producing water-soluble protein-detergent complexes [8]. The stability of these protein-detergent complexes is crucial for protein structural characterization and is significantly influenced by the nature of the detergent molecules/micelles used for protein extraction. Among the numerous detergents available, only a handful have been significant for membrane protein study. Classical detergents such as alkyl glucosides (e.g., OG (*n*-octyl-β-D-glucoside)), maltosides (e.g., DM (*n*-decyl-β-D-maltoside), DDM (*n*-dodecyl-β-D-maltoside)), amine oxides (e.g., LDAO (lauryldimethylamine-*N*-oxide)) and polyoxyethylenes (e.g., tetraoxyethylene glycol monooctyl ether (C_8E_4)) have contributed to structure determination of many membrane proteins [9]. However, due to their canonical architecture of single head and tail groups, these conventional detergents offer limited utility with respect to structurally diverse membrane proteins [10,11]. Thus, development of new amphiphilic agents with distinct architecture is an important area of membrane protein research [12].

The past two decades have witnessed a substantial expansion in the development of amphiphilic systems for membrane protein structural study [13]. Bicelles, nanodiscs (NDs), polymeric amphiphiles (e.g., amphipols (APols) and styrene-maleic acid copolymers (SMAs)) and peptide-based detergents (e.g., lipopeptides and Salipro) have been developed as innovative membrane-mimetic systems [14-19]. Small amphiphilic agents structurally distinct from classical detergents have been also developed, as exemplified by the neopentyl glycol amphiphiles (glucose-neopentyl glycols (GNGs), maltose-neopentyl glycols (MNGs) and neopentyl glycol-derived triglucosides (NDTs)), rigid hydrophobic group-bearing detergents (chobimalt, digitonin, glyco-diosgenin (GDN), lithocholate-based facial amphiphiles (LFAs), terphenyl group-bearing maltosides (TPMs) and facial amphiphiles (FAs)) [20-26]. Recent efforts to implant a new hydrophilic group instead of a typical glucoside/maltoside were made in penta-saccharide-bearing amphiphiles (PSEs) and oligoglycerol detergents (OGDs) [27,28]. Unique hydrophobic groups were introduced into new detergent scaffolds, as exemplified with hemi-

fluorinated surfactants (HFSs) and dendronic trimaltosides (DTMs) [29-30]. Some of these agents have contributed to high resolution structural determinations of membrane proteins via cryo-EM or X-ray crystallographic methods [31-33]. This repertoire highlights the important role of recently-developed small amphiphiles in membrane protein structure determination. However, it is important to note that no one amphiphile system is likely to provide a magic solution for all membrane proteins. In addition, most studies describing new detergent systems lack a detailed analysis of the underlying detergent design principles related to favorable characterization. Such an analysis is essential for future effective detergent development.

The detergent core scaffold used to link detergent head to tail groups can significantly affect detergent properties such as detergent hydrophobic density and micelle size, known to be important for protein solubilization and stabilization [34,35]. Recently developed detergents have rigid core units in many cases, as exemplified by resorcinarene-based amphiphiles (RGAs), calixarene-based detergents (C4Cn), norbornane-based amphiphiles (NBMs), and 1,3,5-triazine-based amphiphiles (TEMs) [36-39]. Although these detergents have been shown to be effective at stabilizing membrane proteins, the rigidity of their core units could limit their conformational flexibility. This in turn might prevent the detergents from forming optimal interactions with a wide range of membrane proteins with diverse structures, preventing the detergents from functioning as universal protein stabilizers. In this work, we have designed a class of maltoside detergents with a flexible core, glycerol-decorated tris(hydroxylmethyl)methane (THM), designated GTMs (Fig. 1). In addition to the flexible core unit, these detergents contain a hydrophobic ethyl (E-GTMs) or a hydrophilic methoxyethoxymethyl (MEM) pendant (M-GTMs) in the central region. When these new detergents were evaluated with several model membrane proteins, some M-GTMs displayed favorable behaviors toward stabilizing the tested membrane proteins compared to DDM (a gold standard detergent) and their hydrophobic versions (E-GTMs). This study demonstrates that the flexible core unit and MEM hydrophilic pendant, when

located together at the detergent hydrophobic-hydrophilic interfaces, allow large conformational changes of the M-GTMs, resulting in enhanced membrane protein stability.

2. Materials and Methods

2.1. MD simulation systems

We modeled two types of homogeneous GTM aggregates consisting of E-GTM-O10 or M-GTM-O10 molecules. The GTM structure preparation, aggregate assembly, and simulation protocols were followed by the CHARMM-GUI *Micelle Builder* and *Membrane Builder* step-by-step protocol [40-42]. The force field parameters for E-GTM-O10 and M-GTM-O10 were generated and assembled by analogy from the CHARMM36 force field [43-46]. In the aggregate systems, 80 E-GTM-O10 and 60 M-GTM-O10 molecules were respectively assembled, and each aggregate system was solvated with the 150 mM KCl bulk solution using TIP3P water model [47]. The initial structure of each GTM aggregate was built as a perfect sphere shape in a cubic box with a length of 128 Å. All simulations were performed using OpenMM-7.4.1 package and the equilibration and production inputs generated by CHARMM-GUI [48,49]. After short minimization and 6-step of equilibrations with gradually decreased positional and sugar dihedral restraint forces (1,875-ps), a 400-ns NPT (constant particle number, pressure, and temperature) production simulation was performed at 303.15 K and 1 bar. Each system was replicated for two independent systems with different initial velocities to improve sampling and check the convergence. The last 100-ns trajectory was used for the analysis. The aggregate radius (R^A) was estimated from the average distance between the center of mass (COM) of the terminal glucose ($\mathbf{R}_T^i$) and the aggregate COM ($\mathbf{R}_{\mathrm{COM}}^A$):

$$R^A = \frac{1}{N}\sum_{i=1}^{N} \langle \sqrt{\left(\mathbf{R}_T^i - \mathbf{R}_{\mathrm{COM}}^A\right)^2} \rangle_t$$

where N = 80 for E-GTM-O10 and 60 for M-GTM-O10.

2.2. Protein stability evaluation

2.2.1 LeuT stability assay.

The hydrophobic amino acid transporter, LeuT, from *Aquifex aeolicus* was purified according to the protocol described previously [50]. We used the cloned LeuT, C-terminally 8xHis-tagged and inserted into the pET16p expression vector. The plasmid was transformed into E. coli C41(DE3) and expression were induced by the addition of 0.1 mM isopropyl β-D-thiogalactopyraniside (IPTG). Cells were harvested by centrifugation after 20 hrs incubation at 20 °C. After isolation of bacterial membranes and solubilization in 1% DDM, LeuT was bound to Ni^{2+}-NTA resin for 1 h and eluted in buffer containing 20 mM Tris-HCl (pH 8.0), 1 mM NaCl, 199 mM KCl, 0.05% DDM and 300 mM imidazole. Subsequently, approx. 1.5 mg/mL protein stock was diluted 10 times into an identical buffer without DDM and imidazole, but supplemented with E-GTM-I/Os, M-GTM-I/Os and DDM at the final concentrations of CMC + 0.04 wt% or 0.2 wt%. Protein samples were stored for 13 days at room temperature. Upon measurement of LeuT activity, 5 µL sample were transferred to a buffer containing 20 mM Tris-HCl (pH 8.0), 200 mM NaCl and the respective test detergent in the concentration. Protein activity was determined by the addition of 20 nM [^{3}H]-leucine and 1.25 mg/mL copper chelate (His-Tag) Ysi beads (scintillation proximity assay (SPA)) [51]. [^{3}H]-Leu binding for the respective samples was measured using a Micro Beta liquid scintillation counter (Perkin Elmer). Non-specific binding was determined in the presence of 10 µM leucine. A similar protocol was used to compare M-GTMs (M-GTM-O11 and M-GTM-O12) with recently developed detergents (LMNG, GNG-3,14, TEM-E10, and TEM-T9) used at 0.2 wt%.

2.2.2 MelB thermos-stability assay.

2.2.2.1. MelB solubilization and thermal stability assay.

E. coli DW2 strain (Δ*melB* and Δ*lacZY*) harboring pK95ΔAHB/WT $MelB_{St}$/CH10 plasmid were used to produce the protein [52,53]. The plasmid contains the gene encoding the wild-type melibiose permease of Salmonella typhimurium ($MelB_{St}$) with a 10-His tag at the C-terminus. Cell growth and membrane preparation were carried out as described [54]. Protein assay was carried out with a Micro

BCA kit (Thermo Scientific). The membrane samples containing $MelB_{St}$ (10 mg/mL) in a solubilization buffer (20 mM sodium phosphate, pH 7.5, 200 mM NaCl, 10% glycerol and 20 mM melibiose) were mixed with individual detergents (DDM, E-GTM-I/Os and M-GTM-I/Os) at 1.5% (w/v). Protein extractions were carried out at 0 °C for 90 min. The resulting samples were further incubated at four different temperatures (0, 45, 55, and 65 °C) for 90 min. Insoluble fractions were removed by ultracentrifugation at 355,590 g in a Beckman OptimaTM MAX Ultracentrifuge using a TLA-100 rotor for 45 min at 4 °C. 20 μg membrane proteins without ultracentrifugation and equal volume of detergent extracts after the ultracentrifugation step were loaded for analysis by SDS-15% PAGE, and $MelB_{St}$ was visualized by immunoblotting with a HisProbe- HRP antibody (Thermo Scientific).

2.2.2.2 MelB Trp→D^2G FRET assay.

RSO membrane vesicles were prepared via osmotic lysis from *E. coli* DW2 cells containing $MelB_{St}$ or $MelB_{Ec}$ [54,55]. The RSO membrane vesicles in a buffer containing 100 mM KPi (pH 7.5) and 100 mM NaCl at a protein concentration of 1 mg/ml were treated with 1.0 % individual detergents (DDM and M-GTM-I10/11 and M-GTM-O10/11) at 23 °C for 60 min and subjected to ultracentrifugation using TLA 120.2 rotor at >300,000 g for 45 min at 4 °C. The supernatants were applied for the FRET (Trp→D^2G) experiments using an Amico-Bowman Series 2 (AB2) Spectrofluorometer. The 2'-(*N*-Dansyl)aminoalkyl-1-thio-β-D-galactopyranoside (D^2G, dansylgalactoside) was obtained from Drs. Gerard Leblanc and H. Ronald Kaback. D^2G FRET signal was collected at 490 and 465 nm for $MelB_{St}$ and $MelB_{Ec}$, respectively, upon excitation of Trp residues at 290 nm [56]. 10 μM D^2G and excess melibiose or equal volume of water (control) were added into the MelB solutions at 1-min and 2-min time points, respectively. Apparent K_d values of D^2G and melibiose for $MelB_{St}$/$MelB_{Ec}$ have previously been reported to be 10.35/3.10 μM and 1.07/0.49 mM in the presence of Na^+ [54].

2.2.3 β_2AR stability assay.

β_2AR was purified using 0.1% DDM as previously described [57,58]. Briefly, the receptor was expressed in Sf9 insect cells infected with baculovirus and solubilized in 1.0 % DDM. The DDM-solubilized

receptor was purified by alprenolol sepharose in the presence of 0.01% cholesteryl succinate (CHS). The DDM-purified β_2AR (1.0 μM) was diluted 150-fold using buffer solutions containing individual detergents (DDM, E-GTM-I10/I11/I12, E-GTM-O10/O11/O12, M-GTM-I10/I11/I12, M-GTM-O10/O11/O12) to reach detergent concentrations of 0.2 wt%. β_2AR in each detergent was stored for 5 days at room temperature and its ligand binding capacity was measured at regular intervals by incubating the receptor with 10 nM of radioactive [^{3}H]-dihydroalprenolol (DHA) for 30 min at room temperature. The mixture was loaded onto a G-50 column and the flow-through with a small amount of binding buffer (20 mM HEPES pH 7.5, 100 mM NaCl, supplemented with 0.5 mg/mL BSA) was collected. A further 15 mL scintillation fluid was added. Receptor-bound [^{3}H]-DHA was measured with a scintillation counter (Beckman). Receptor stability was assessed by measuring the ligand binding ability at regular intervals during the incubation period.

2.2.4 MOR stability assay

MOR was purified as previously reported [59]. To perform the long-term stability assay, MOR stock solution (2 μM) in 0.05 % DDM was diluted 100-fold using buffer solutions (20 mM HEPES pH 7.5, 100 mM NaCl) containing individual detergents (M-GTM-I/Os, LMNG, and DDM) to give final receptor concentration of 20 nM and individual detergent concentrations of 0.1%. MOR in each detergent was stored for 6 days at 4 °C and its specific ligand binding capacity was measured by incubating the receptor with 30 nM of radioactive [^{3}H]-diprenorphine (DPN) for 60 min at room temperature. The non-specific binding was measured by incubating the receptor with 30 nM [^{3}H]-DPN and 100 μM Naloxone for 60 min at room temperature. After incubation the mixture was loaded onto Zeba™ 96-well Spin Desalting Plates, 40K MWCO. The flow-through that contains ligand-bound receptor was collected through centrifugation. After adding 5 mL scintillation fluid the radioactivity was measured with a scintillation counter (Beckman). For each detergent we have three specific binding groups and one non-specific binding group. The final binding capacity was calculated by subtracting the radioactivity of non-specific group from specific groups.

2.3. *Statistical Analysis*

The experiments were repeated at least twice as presented in individual figure captions. All data are presented in terms of mean ± standard error of the mean (SEM) or standard deviation (SD). Detergent efficacy for long-term protein stabilization was compared by calculating 'area under curve' from the time-dependent protein stability results. The resulting 'area under curve' data was analyzed using one-way ANOVA followed by Dunnett's multiple comparisons test. This statistical test was also applied for the temperature-dependent $MelB_{St}$ solubilization. Statistical analysis was performed with GraphPad 6.0 software.

3. Results

3.1. *Detergent structures, physical characterizations and molecular dynamics simulations*

Detergent flexibility is a key parameter for effective encapsulation of membrane proteins with diverse structures, as it allows the detergent head and tail groups to favorably interact with the irregular surfaces of membrane proteins. This explains why conventional detergents with a flexible alkyl chain such as DDM, DM and OG are widely used for membrane protein manipulation. A detergent linker often introduced to connect detergent head with tail group in a detergent design can significantly modulate the flexibility of detergent molecules. The GTMs introduced here have a flexible core unit comprising THM and glycerol (i.e., glycerol-decorated THM), distinct from previous detergent examples with rigid ring structures in the linking regions (Fig 1A) [34-39]. The flexible core of the GTMs would be beneficial for membrane protein stability due to the ability to vary detergent conformation according to the architecture/dimensions of target proteins, resulting in favorable *detergent-protein* interactions in the micellar environments. It is important to point out that the rigid hydrophobic group-bearing detergents can also be effective for protein stability, as exemplified by digitonin and GDN [24]. The enhanced protein stabilization properties of digitonin and GDN, however, have a different basis than that of the flexible core-bearing GTM detergents. Due to the presence of a hydrophobic group

with both high hydrophobic density and a planar-like architecture, these diosgenin-based detergents favor *detergent-detergent*. Thus, the GTMs which favour *detergent-protein* interactions are likely to play a distinctive role in membrane protein structural study. Inspired by natural lipid molecules, the glycerol unit was used as a linker to connect detergent head and tail groups (three maltose units and three alkyl chains, respectively), while the THM core unit was utilized to introduce two different pendants, hydrophobic (ethyl) and hydrophilic (methoxyethoxymethyl; MEM) chains (Fig 1B,C). The pendant chain is conjugated into the central carbon of the THM unit, thereby located at the interface between the hydrophilic and hydrophobic groups. To reflect the chemical structures of the head group (maltoside), the detergent core unit (glycerol-decorated THM) and the pendant (ethyl/MEM chain), the new detergents were designated as E- (ethyl) or M (MEM)–GTMs (Fig 1D,E). Each set of GTMs can be further divided into two subsets depending on the relative positions of the head and tail groups (Scheme 1). For one subset (GTM-Is), the maltoside head group and alkyl chains were conjugated to the inner and outer hydroxyl groups (2°-OH and 1°-OH) of the glycerol units, respectively, while this arrangement was switched in the case of the other subset (GTM-Os). Thus, 'I' or 'O' in the detergent designations indicates the relative position (inner or outer) of the glycerol hydroxyl group used to connect the maltoside head group. Consequently, the new detergents share glycerol-decorated THM as the core unit, but vary in pendant polarity (ethyl/MEM) as well as the arrangement of the detergent head and tail groups, producing four sets of GTMs (E-GTM-Is/Os and M-GTM-Is/Os). The alkyl chain (i.e., main chain) length of the new detergents varied from C10 to C12, as incorporated in detergent designation (Scheme 1). The chain length variation is necessary to find a detergent having the optimal balance between detergent hydrophilicity and hydrophobicity (i.e., hydrophile-lipophile balance (HLB)) for protein stability [60,61]. In addition, detergent chain length is crucial for compatibility of detergent molecules with the hydrophobic surface dimensions of membrane proteins.

<Figure 1>

Thanks to high conformational flexibility of the detergent core unit (i.e., glycerol-decorated THM), the hydrophobic ethyl pendant in the GTM architecture is likely placed in the central part of the hydrophobic space formed by the three alkyl chains in aqueous solution (Figure 1B,D). In contrast, the hydrophilic MEM pendant of the M-GTMs would direct toward the hydrophilic rather than the hydrophobic region and occupy the central part in the hydrophilic space formed by the three maltoside groups (Figure 1C,E). Thus, the variation in the pendant chain from the hydrophobic to hydrophilic group likely induces a large conformational change in the core region of the new detergents, resulting in a significant difference in molecular geometry between two sets of GTMs. Based on the direction of the pendant chain, the E-GTMs should have a truncated conical shape in aqueous environments, while the M-GTMs would be close to a conical shape in molecular geometry. Accordingly, it was anticipated that the E-GTMs with the large hydrophobic volumes form large self-assemblies, while self-assemblies formed by the M-GTMs with a large hydrophilic volumes are small [62,63]. In previous studies, detergent self-assembly size was controlled by rather obvious variations in detergent structures such as detergent alkyl chain length and head group identity (glucose/maltose) [32,33], but the current design suggests a new way to effectively change detergent self-assembly size, through the introduction of pendant chains with different polarity into a flexible detergent core.

<Scheme 1>

The E- or M-GTMs were prepared from inexpensive starting materials via efficient protocols comprising three or five synthetic steps (Scheme 1). The preparation of the GTM-Is started with an epoxide ring opening reaction of an ethyl/MEM pendant-bearing triglycidyl ether (**A1**) with an alkoxide under basic conditions (~68% yield). Attack of a nucleophilic alkoxide to the less sterically hindered carbon of the epoxide ring produced a trialkylated triol derivative (**B**) with the three alkyl chains

connected to the outer hydroxyl groups (1°) of the glycerol unit. The inner hydroxyl groups (2°) generated by the alkoxide attack were utilized for the introduction of the maltoside head groups *via* glycosylation (~65% yield). The resulting glycosylated products were subjected to a global deprotection to produce the inner maltoside versions (GTM-Is) (~90% yield). The regio-isomeric detergents of these inner maltoside versions (GTM-Os) were prepared from the glycerol-decorated THM compound with the ethyl/MEM pendant (**A2**). Following a selective protection of the outer hydroxyl groups (1°) of **A2** with TBDMS (~74% yield), the main alkyl chains were conjugated to the inner hydroxyl groups (2°) of the glycerol unit, followed by TBAF-promoted TBDMS removal (~57% yield in two steps). The resulting trialkylated triol derivatives (**C**) were used for glycosylation and a global deprotection to yield the outer maltoside versions (GTM-Os) (~65 and ~90%, respectively). All the glycosidic bonds formed in the glycosylation are likely to have β-configuration in their stereochemistry due to the involvement of neighboring benzoyl group in the formation of a cyclic oxocarbenium ion intermediate. This β-selectivity was confirmed by the ^{1}H NMR spectra of the individual detergents. For instance, the NMR spectrum of E-GTM-O11 showed two separated signals at 4.31 and 5.16 ppm, assigned to the β-and α–anomeric protons (H_β and H_α), respectively (Fig. 3Sa). Coupling constants (^{3}J) of these α– and β-anomeric peaks (4.0 and 8.0 Hz, respectively) are also consistent with their stereochemistry. The same chemical shifts (δ) and coupling constants (^{3}J) were observed for M-GTM-O11 (Fig. 3Sb). In the cases of inner maltoside versions (E-GTM-I11 and M-GTM-I11), we observed the α–anomeric signals at a similar chemical shift (5.18 ppm), but the β-anomeric peaks of these inner versions appeared at ~ 4.50 ppm instead of 4.31 ppm (Fig 3Sc,d). The conjugation of the maltoside group to the secondary rather than the primary hydroxyl group explains this downfield shift of the β-anomeric signals observed for the inner maltoside versions. In addition, the presence of the neighboring stereo-chemically ill-defined carbons, as indicated by the wavy lines in the chemical structures of the GTM-Is (Scheme 1), makes the β-anomeric signals of these versions more complex than those of their outer counterparts. The 2D NOESY spectra of E-GTM-O11 and M-

GTM-O11 allowed us to further confirm the β-glycosidic bond formation (Fig. 2). Due to the close proximity in space, a strong NOE correlation signal was detected between the β-anomeric proton (H_β) and the proton (H_1). The α-anomeric proton (H_α) strongly correlates to the glycerol proton (H_2), indicating the connection of the maltoside group to the terminal alcohol of the glycerol unit; these detergents are the outer versions of GTMs. In the case of M-GTM-O11, we observed a strong correlation between two protons on the MEM pendant (H_3 and H_4), which was not found in the NOESY spectra of the ethyl pendant version (*i.e.*, E-GTM-O11). Instead, E-GTM-O11 showed correlation signals between the protons of the ethyl pendant (H_3 and H_4) and the proton of the THM unit (H_9) (Fig. 4S). Of note, the prepared GTMs are mixtures of diastereomers which can be beneficial for protein stabilization as the subtle structural variation can facilitate the formation of detergent assemblies adaptable to irregular protein surfaces.

<Figure 2>

The water-solubility of the GTMs profoundly varied depending on the polarity of the pendant group. The C10 alkyl-chained E-GTMs were 10 wt% soluble in water, but a further increase in alkyl chain length decreased detergent water-solubility. The C11 and C12 versions of E-GTMs were ~5% and ~1 (outer)/3% (inner) water-soluble, respectively. In contrast, all M-GTMs with the hydrophilic pendant (*i.e.*, MEM) gave sufficient water-solubility (> 10 wt%) partly due to the increased hydrophilicity. Self-assembly behaviors of the GTMs are also significantly affected by the pendant polarity. Critical aggregation concentrations (CACs) of the GTMs, estimated using a fluorescent dye (diphenylhexatriene (DPH)) [64], were low compared to that of DDM (1.5~10 *vs* 170 μM), indicating the high propensity of the new detergents to self-associate and the high thermodynamic stability of their self-assemblies. Due to the presence of the hydrophilic MEM instead of the hydrophobic ethyl pendant, the M-GTMs are expected to give high CACs relative to the E-GTM counterparts due to the

reduced hydrophobicity of the lipophilic groups. However, little difference in CACs was observed between these two sets (E- and M-GTMs), implying that the M-GTMs have a molecular geometry more effective for aggregate formation than the E-GTM counterparts. In terms of the regio-isomeric GTMs, the outer maltoside versions (GTM-Os) are expected to give lower CACs than the inner counterparts (GTM-Is) due to the short inter-alkyl chain distance (*i.e.*, increased alkyl chain density in the hydrophobic region). Note that the alkyl chains were connected to the inner hydroxyl groups of the core unit (*i.e.*, glycerol-decorated THM) for the GTM-Os, while the alkyl chains of the GTM-Is were conjugated to the outer hydroxyl groups. As expected, the GTM-Os gave lower CACs than the equivalent GTM-Is, but their CAC differences were rather small, particularly for the M-GTMs. This is likely due to a minor difference in the inter-alkyl chain distances between the outer and inner GTMs than it appears, originating from the flexible nature of the detergent core.

Table 1 Molecular weights (MWs), critical aggregation concentrations (CACs), and water-solubility of new detergents (E-GTMs and M-GTMs), and hydrodynamic diameters (D_h; n = 4) of their aggregates formed in water at room temperature.

Detergent	MW[a] (Da)	CAC (μM)	D_h (nm)[b]	Solubility (wt%)
E-GTM-I10	1750.1	10	32.8 ± 0.4	~10
E-GTM-I11	1792.1	3.0	62.8 ± 0.2	~5
E-GTM-I12	1834.2	1.5	76.0 ± 0.6	~3
E-GTM-O10	1750.1	5.0	47.0 ± 0.4	~10
E-GTM-O11	1792.1	2.0	77.8 ± 0.2	~5
E-GTM-O12	1834.2	1.5	85.6 ± 1.4	~1
M-GTM-I10	1810.1	6.0	9.2 ± 0.4	~10
M-GTM-I11	1852.2	5.0	22.2 ± 4.0	~10
M-GTM-I12	1894.3	4.0	35.4 ± 1.6	~10
M-GTM-O10	1810.1	5.0	7.6 ± 0.2	~10

M-GTM-O11	1852.2	4.0	12.6 ± 0.2	~10
M-GTM-O12	1894.3	3.0	33.6 ± 0.6	~10
DDM	510.6	170	6.8 ± 0.6	~10

[a] Molecular weight of detergents. [b] Hydrodynamic diameter of detergent self-assemblies measured at 1.0 wt% by dynamic light scattering experiments.

In order to further investigate the effect of detergent pendant polarity (E-GTMs vs M-GTMs) or detergent regio-chemistry (GTM-Os vs GTM-Is) on their self-assemblies, the hydrodynamic diameters (D_h) of the aggregates were measured by dynamic light scattering (DLS) experiments. A large difference in aggregate size was observed depending on the pendant polarity. The D_h values of aggregates formed by M-GTM-I10, M-GTM-I11 and M-GTM-I12 were 9.2, 22.2 and 35.4 nm, respectively, substantially smaller than the E-GTM counterparts (E-GTM-I10 (32.8 nm), E-GTM-I11 (62.8 nm) and E-GTM-I12 (76.0 nm)). A similar trend was observed for the M-GTM-Os versus E-GTM-Os. This is due to a large change in detergent geometry from a truncated conical to a conical shape when the pendant is converted from the hydrophobic ethyl to the hydrophilic MEM chain, as described above. In contrast, the inner and outer maltoside versions (GTM-Is and GTM-Os, respectively) gave an only minor differences in the size of their aggregates.

<Figure 3>

Based on the relative location of the head and tail groups, the GTM-Os are expected to form smaller aggregates than the GTM-Is. This trend was indeed observed for the M-GTMs, but the opposite trend was observed for the E-GTMs; the E-GTM-Os form larger aggregates than the E-GTM-Is. Therefore, the conformational changes of the detergent molecules that result from the variation in pendant polarity are a key determinant for the physical properties of detergents or detergent self-assemblies such as water solubility, CACs and aggregate sizes. In contrast, detergent regio-chemistry (*i.e.*, the relative

location of the head and tail groups) has little effect on those detergent properties. The physical differences between the E- and M-GTMs could also result from a change in overall HLB between the two series; however, this latter seems unlikely because the difference between ethyl and MEM is relatively small in the context of the large GTM molecules. When we analyze the populations of detergent aggregates in terms of their sizes, the aggregates formed by M-GTM-O11 showed a narrow distribution compared to those formed by the E-GTM-O11 (Fig. 3a,b). This was a general trend for all GTMs, indicating that self-assemblies formed by the M-GTMs have higher homogeneity than those formed by the E-GTMs (Fig. S1 & S2). Detergent self-assemblies were further investigated with a variation in detergent concentration. Self-assemblies formed by E-GTM-O11 were gradually enlarged with increasing detergent concentration from 0.3 to 2.0 wt% (Figure 3c). Similar behavior was observed for self-assemblies formed by M-GTM-O11. Detergent self-assemblies were further characterized in terms of their temperature-dependent size variation (Figure 3d). Both E-GTM-O11 and M-GTM-O11 tend to form large aggregates with increasing solution temperature. The aggregate size (D_h) increased from 67.6/9.7 to 79.4/25.8 nm for E/M-GTM-O11 when solution temperature was elevated from 15 to 65 °C.

Pendant polarity-dependent detergent conformations and self-assembly architectures were further explored by performing molecular dynamics (MD) simulations of aggregate systems formed by E-GTM-O10 and M-GTM-O10. To simplify these simulations, we fixed the stereochemistry of the stereochemically ill-defined carbons within the glycerol units as the *R* configuration, and used 80 and 60 molecules for E-GTM-O10 and M-GTM-O10, respectively, for aggregate formation. These aggregation numbers were approximated from their number-weighted DLS profiles (Figs. S1 & S2). At the early stage of the simulation, both initially sphere-shaped aggregate structures were gradually transformed into bicelle-like architecture (Figs. 4A,B & S5). These structural changes in the detergent aggregates seem to occur to fill cavities initially present in the spherical micelle centers. Aggregate structures formed by E-GTM-O10 and M-GTM-O10 were analyzed in terms of radial densities of different

molecular components (*i.e.*, alkyl chains, glycerol-decorated THM core, maltoses, pendant chain) from the center of mass (COM) of each aggregate (Fig. S5). Each molecular component of the GTMs shows a broad radial distribution, further supporting a bicelle-like aggregate structure rather than a micellar-like structure. The two pendant groups of E-GTM-O10 and M-GTM-O10 are also distributed broadly, but the hydrophobic ethyl pendant of E-GTM-O10 is placed in the central region of the aggregates than the THM core unit, while the hydrophilic MEM pendant of M-GTM-O10 is distributed in the outer region than the core unit, indicating different directions of the pendants depending on their polarity (Fig. S6). The direction of the pendant in E/M-GTM was quantitatively characterized by measuring angles between three points: the self-assembly COM, THM center carbon, and last carbon of the pendant (Fig. 4C-E). Clearly, the ethyl pendants of E-GTM-O10 mostly show three-point angles larger than 90°, indicating that the hydrophobic pendants are positioned toward the aggregate COM. In contrast, the hydrophilic pendants of M-GTM-O10 mostly show three-point angles less than 90°, suggestive of the direction of the MEM pendant toward the outer region. These pendant directions obtained from the MD simulations corroborate our hypothesis on pendant polarity-dependent change in pendant direction. The MD simulations also allowed us to gain an insight into the molecular geometry of the GTMs. When we investigated detergent conformations by overlaying individual GTM monomers using the last 100-ns trajectory, we found wider separations between the maltoside head groups for M-GTM-O10 compared to E-GTM-O10 located in the central region of the aggregates (Figs. 4F,G & S7). As for the detergent alkyl chains, an opposite trend was observed; the detergent alkyl chains of M-GTM-O10 are less separated from each other than those of E-GTM-O10. This trend was also observed for detergent monomers at the edge of the aggregates, although it was not as obvious as at the center region. The high alkyl chain density of M-GTM-O10 relative to that of E-GTM-O10 was further supported by quantitative analysis of the alkyl chain density of these two detergents (Fig S8). The analysis shows that aggregates formed by M-GTM-10 have higher alkyl chain density than those formed by E-GTM-O10 in their hydrophobic regions (5 to 20 Å from the aggregate COM). A reverse

trend was found in the hydrophilic region of the aggregates (25 to 45 Å from the COM). The relative separation between detergent head/tail groups described here is consistent with pendant polarity-based detergent conformations in their aggregates described above. Of note, these overlaid views clearly show the opposite direction of two pendants of E- and M-GTMs (ethyl and MEM) (Figs. 4F,G). The radii (R^A) of the E-GTM-O10 and M-GTM-O10 aggregates, estimated from the average distance between the COM of the terminal glucose and the aggregates COM, are 35.97 Å (±0.12) and 32.72 Å (±0.27), respectively. These calculated values are more or less comparable to the aggregate sizes obtained from the DLS experiments (Figs. S1a & S2a), strengthening the reliability of the MD simulations.

<Figure 4>

3.2. *Detergent evaluation with a set of membrane proteins*

The GTMs were first evaluated with an ion-coupled transporter from the bacterium *Aquifex aeolicus*, the hydrophobic amino acid transporter, LeuT [65]. This transporter is a prokaryotic homologue of human neurotransmitter transporters belonging to the neurotransmitter: sodium symporter (NSS) family. LeuT was expressed in *E. coli* and extracted from the membranes with 1.0 wt% DDM, immobilized on a Ni^{2+}-NTA resin, washed and eluted with imidazole into a buffer containing 0.05 wt% DDM. DDM were exchanged with the individual GTMs by dilution into final GTM concentrations of CMCs +0.04 wt%. Protein stability in the different GTMs were assessed as the ability of LeuT to bind the radiolabeled substrate ([^{3}H]-leucine (Leu)) [51,66]. The substrate binding ability of the transporter was monitored regularly over the 13-day incubation at room temperature. The DDM-solubilized LeuT showed a steady decrease in the substrate binding ability over time. The worst result was obtained with E-GTM-O10 which resulted in the loss of almost all [^{3}H]-Leu binding activity after a 6-day incubation (Fig. S9a). The other E-GTMs, particularly E-GTM-I10/I11/O11, were markedly better than

DDM at stabilizing the transporter long term (Fig. S9c and Table S1). Interestingly, the transporter in the long alkyl-chained detergents (E-GTM-O12/I12) gave rather low initial leucine binding, but this initial activity was retained over the entire incubation period. When detergent concentration was increased to 0.2 wt%, a similar trend was found with E-GTM-O12/I12. This C12 alkyl-chained E-GTM-solubilized LeuT showed rather low initial substrate binding ability, but that initial activity was little decreased over time (Fig. S9b). LeuT solubilized in the other E-GTMs (E-GTM-I10, E-GTM-I11, E-GTM-O10, and E-GTM-O11) showed higher levels of Leu binding than DDM over the incubation period (Figure S9d and Table S2). It is interesting to note that, despite the same alkyl chain length, the two regio-isomeric GTMs (*i.e.*, E-GTM-I10 and E-GTM-O10) showed a large difference in retaining the substrate binding ability of the transporter (Tables S1 and S2). When the hydrophilic pendant-bearing detergents (M-GTMs) were used, all new agents yielded high initial protein activity even in the cases of long alkyl chained detergents (M-GTM-O12/I12) (Fig. 5). Furthermore, protein activities in the individual M-GTMs were fully maintained over the 13-day incubation period, demonstrating the superior nature of the M-GTMs compared to DDM for LeuT stability (Fig. S10 and Table S3). Thus, the pendant change from the ethyl to the MEM chain dramatically rescued detergent efficacy of the poorly-behaving E-GTMs (E-GTM-O10 and E-GTM-I12), highlighting the favorable architecture of the M-GTMs compared to that of the E-GTMs for LeuT stability (Table S4).

<Figure 5>

The new detergents were further tested with another model transporter, melibiose permease, a prokaryotic symporter of *Salmonella typhimurium* ($MelB_{St}$) [54-56,67]. For initial screening, *E. coli* membrane fragments containing $MelB_{St}$ were incubated with DDM or the individual GTMs at 1.5 wt% for 90 min at 0 °C. Following ultracentrifugation, the amounts of soluble $MelB_{St}$ in the supernatant were separated and visualized by SDS-PAGE and Western blot, respectively. The C11 or C12 alkyl-

chained E-GTMs (E-GTM-O11, E-GTM-O12, E-GTM-I11 and E-GTM-I12) failed to extract measurable amounts of the transporter, probably due to their limited water-solubility. The C10 alkyl-chained E-GTMs (E-GTM-I10 and E-GTM-O10) and all the M-GTMs extracted $MelB_{St}$ in reasonable amounts, but all GTMs except M-GTM-I10 and M-GTM-O10 were rather inferior to DDM for MelB extraction efficiency (Fig. 6a and Table 5). Based on these data, all M-GTMs as well as E-GTM-I10 and E-GTM-O10 were further investigated by incubating detergent-extracted $MelB_{St}$ at an elevated temperature (45, 55, or 65 °C) for another 90 min. This temperature variation study informs how effective each detergent is at preventing protein aggregation under the conditions tested. When the transporter samples were incubated at 45 °C, the amounts of soluble $MelB_{St}$ for each GTM tend to increase compared to that obtained at 0 °C, probably due to enhanced membrane dynamics or increased detergent solubility at this elevated temperature (Fig. 6a). With a further increase in incubation temperature to 55 °C, there was little DDM-solubilized $MelB_{St}$ detectable. The long alkyl-chained M-GTMs (M-GTM-I12/O12) also yielded small amounts of soluble $MelB_{St}$. However, the other GTMs tested here were more effective than DDM at retaining $MelB_{St}$ in a soluble state, with the best efficacy observed for M-GTM-O10/O11 (Table S6). These MEM-bearing detergents retained ~70% $MelB_{St}$ in a soluble state. The superiority of the M-GTMs to E-GTMs detected in this study is in good agreement with the results obtained with LeuT. M-GTM-I10 and M-GTM-O10 were substantially more effective than the ethyl counterparts (E-GTM-I10 and E-GTM-O10, respectively) at retaining $MelB_{St}$ solubility (Table S6). On the basis of the superior performance compared to the E-GTMs, representative M-GTMs (M-GTM-I10/I11 and M-GTM-O10/O11) were selected for MelB functional study. MelB functionality was monitored by sequential addition of two galactosides, 2'-(*N*-dansyl)aminoalkyl-1-thio- β-D-galactopyranoside (D^2G) and melibiose, into detergent-extracted protein samples [68]. Due to efficient energy transfer from the indole ring of tryptophan residue to the dansyl unit of the fluorescent ligand bound to the active site, active $MelB_{St}$ gives rise to a strong fluorescence emission in the presence of D^2G. The subsequent addition of non-fluorescent melibiose in excess displaces D^2G

in the active site, resulting in a reduction in fluorescence intensity. Thus, this melibiose reversal of Förster resonance energy transfer (FRET) assay can be used to effectively estimate the ability of the detergents to maintain MelB function. The fluorescence signal of DDM-solubilized $MelB_{St}$ is responsive to the successive addition of D^2G and melibiose. Specifically, the fluorescence signal increased and decreased upon additions of first D^2G and subsequently melibiose, respectively (Fig. 6b). However, no response was observed when a less stable homologue, MelB obtained from *E. coli* ($MelB_{Ec}$), was used under the same conditions [74]. In contrast, all the M-GTMs tested here provided relevant changes in the fluorescence signals of both transporters ($MelB_{St}$ and $MelB_{Ec}$) under the same conditions. Thus, it can be concluded that the GTMs (M-GTM-O10/11 and M-GTM-I10/11) tested here are reasonably efficient at protein extraction and, more importantly, are effective at maintaining MelB structural integrity.

<Figure 6>

The superior efficacy for LeuT and MelB stabilization encouraged us to further evaluate the GTMs for stabilization of G-protein coupled receptors (GPCRs), major pharmaceutical targets. For this purpose, human β_2 adrenergic receptor (β_2AR) was first isolated in DDM [57]. The resulting DDM-purified receptor was subjected to detergent exchange by diluting into buffer solutions supplemented with the individual GTMs. At a detergent concentration of 0.2 wt%, protein stability was assessed by measuring receptor ability to bind the radio-active antagonist ([^{3}H]-dihydroalprenolol (DHA)) at room temperature [70]. All GTMs except two C12 alkyl-chained E-GTMs (E-GTM-O12 and E-GTM-I12) were effective at stabilizing the receptor (Fig. S11). Detergent evaluation was further carried out with the selected detergents (E-GTM-O10/O11/I10/I11 and M-GTM-O10/O11/O12/I10/I11/I12). The ligand binding ability of the receptor in these individual detergents was regularly monitored over a 5-day incubation at room temperature (Figs. 7a and S13a). All the tested GTMs were more effective than

DDM at maintaining the DHA binding ability of the receptor over the test period, with the best performance observed for M-GTM-O12 (Figs. S12a and 13b; Table S7). This hydrophilic pendant-bearing detergent retained ~ 80% initial ligand binding of the receptor after the 5-day incubation. Detergent efficacy for receptor stabilization tends to enhance with increasing alkyl chain length among the tested detergents, particularly for the M-GTMs. The C12 versions of the M-GTMs (M-GTM-I12 and M-GTM-O12) were the most effective of each set at receptor stabilization, followed by the C11 and C10 versions (Fig. S12a and Table S7). When two regio-isomeric detergents were compared, there was little clear difference in detergent efficacy for preserving receptor integrity.

<Figure 7>

The marked ability to stabilize LeuT, $MelB_{St}$ and β_2AR prompted us to select the M-GTMs for evaluation with another GPCR, mouse μ-opioid receptor (MOR) [71]. DDM-purified receptor was diluted into the individual M-GTM-containing buffer solutions for detergent exchange. Long-term receptor stability was assessed by measuring the ability of MOR to bind the radio-active antagonist ([^{3}H]-diprenorphine (DPN)) over the course of a 3-day incubation at room temperature [72]. DDM-solubilized receptor gave a complete loss in ligand binding ability after a 1-day incubation, indicating that this GPCR is more challenging to stabilize than β_2AR. The C10 and C11 versions (M-GTM-I10/O10 and M-GTM-I11/O11) of the tested detergents were clearly better than DDM at preserving the DPN binding ability of the receptor (Figure S12b and Table S8), but their efficacies may not insufficient for downstream characterization of the receptor. An increase of the alkyl chain length to C12 failed to give further enhancement in detergent efficacy in the case of the inner maltoside version (M-GTM-I12), but M-GTM-O12 yielded a full retention in receptor stability over the 3-day incubation. The overall tendency of the M-GTMs to enhance detergent efficacy with increasing alkyl chain length was consistent with the β_2AR result; M-GTM-O12 was most effective, followed by M-GTM-O11 and M-

GTM-O10 for the stabilization of both GPCRs (Figure S12b and Table S8). In addition, M-GTM-O10 and M-GTM-O12 were better than the inner counterparts (M-GTM-I10 and M-GTM-I12, respectively) at stabilizing both receptors long term (Figure S12b and Table S8). Importantly, the best GTM (i.e., M-GTM-O12) was even more effective than LMNG, a significantly improved detergent for GPCR stability, at stabilizing the receptor (Figure S12b and Table S8). Combined together, the result indicates that M-GTM-O12 holds significant potential for GPCR structural study. The selected GTMs (M-GTM-O11 and M-GTM-O12) were further evaluated at 0.2 wt% for LeuT stability to compare their efficacy with some of recently developed detergents (GNG-3,14, TEM-E10 and TEM-T9) [39,73]. Consistent with previous results, these recently developed detergents were better than DDM for LeuT stability and were more or less comparable to LMNG (Figure S14 and Table S9). Remarkably, the tested GTMs (M-GTM-O11 and M-GTM-O12) were even more effective than LMNG and the recently developed detergents at stabilizing the transporter (Figure S14 and Table S9).

4. Discussion

We have prepared four sets of pendant-bearing maltoside detergents (GTMs) with the glycerol-decorated tris(hydroxymethyl)methane (THM) unit in the core region that vary in terms of pendant polarity as well as the relative position of the head and tail groups. When evaluated with four model membrane proteins (LeuT, MelB, β_2AR and MOR), the new detergents showed a large variation in their efficacy for protein stabilization depending on the model membrane protein tested. For instance, E-GTM-O10 was rather poor at stabilizing LeuT, but this C10 version was effective at stabilizing MelB and β_2AR. In addition, M-GTM-O12 was superior to DDM at stabilizing LeuT, β_2AR and MOR, while this C12 alky-chained detergent appeared to be inferior to DDM at stabilizing MelB. Detergent alkyl chain length optimal for protein stability was dependent on the tested membrane protein. The C10/C11 versions were most effective at stabilizing LeuT and $MelB_{St}$, while the C12 versions of the M-GTMs were best in stabilizing β_2AR and MOR. The protein-specific nature of detergent efficacy observed here, consistent

with the general notion that there is no single solution for all membrane proteins, is a natural consequence of a large range of diversity in protein structures and functions. Variations in both the dimensions of protein hydrophobic/hydrophilic surfaces and the tendency of a specific protein to aggregate/denature are likely responsible for the protein-dependent detergent efficacy. Thus, it is challenging to develop a single detergent effective with multiple membrane proteins. DDM is a gold standard as it is the most effective conventional detergents at stabilizing many membrane proteins, as illustrated by the wide use of this maltoside in membrane protein manipulation [9,74]. The current study is valuable as we identified several new agents markedly more effective than the gold standard DDM at stabilizing every membrane protein tested here. Of the E-GTMs, only E-GTM-I10 showed an enhanced efficacy compared to DDM for the stabilization of some membrane proteins tested here, but even this detergent failed to give a significantly enhanced efficacy for β_2AR stabilization. In contrast, most MEM pendant-bearing detergents (M-GTMs) were clearly superior to DDM at stabilizing the membrane proteins tested. In particular, M-GTM-O10/O11/I11 were significantly more effective than DDM at stabilizing all the tested membrane proteins and thus these detergents should have wide applicability for membrane protein manipulation. On the other hand, some detergents showed a marked preference for a particular class of membrane proteins. For instance, M-GTM-I10 was especially effective at stabilizing the two transporters (LeuT and MelB), while M-GTM-O12 was most effective at stabilizing the two GPCRs (β_2AR and MOR). These results highlight that M-GTM-I10 and M-GTM-O12 have potential for structural study of transporters and GPCRs, respectively. When M-GTM-O12 was also shown to be superior to LMNG at stabilizing MOR. The same conclusion can also be reached for β_2AR stability when detergent efficacy was compared based on previous results reported in literatures [38,39]. When further compared with recently developed detergents, M-GTM-O11 and M-GTM-O12 were more effective than GNG-3,14, TEM-E10 and TEM-T9 at maintaining LeuT stability long term.

The comparative study of the new detergents in terms of pendant polarity and the relative position of the detergent head and tail groups allowed us to pinpoint detergent structural features responsible for membrane protein stabilization. The overall superior property of the M-GTMs relative to the E-GTMs generally observed with all the tested membrane proteins likely correlates with the dramatic conformational change resulting from the pendant variation (ethyl *vs* MEM). The conversion of the hydrophobic (ethyl) to hydrophilic pendant (MEM) in the detergent hydrophilic-hydrophobic interfaces changes the pendant direction from the hydrophobic to the hydrophilic side in the aqueous environments. This conformational change, as supported by the MD simulations on detergent aggregates, likely leads to a decrease in detergent inter-alkyl chain distance, thus increasing alkyl chain density (*i.e*., hydrophobic density) in the interior of self-assemblies formed by the M-GTMs. The physical data of the M-GTMs such as the relatively low CACs and small aggregate sizes are supportive of their high hydrophobic density in detergent assemblies. It is worth mentioning that the conformational change of the GTMs dependent on the pendant polarity is enabled by the use of the flexible linker (i.e., the glycerol-decorated THM unit) in the detergent core region. Thus, hydrophilicity of the MEM pendant and flexibility of the detergent core unit cooperatively contribute to the marked efficacy of the M-GTMs for protein stabilization compared to the E-GTMs/DDM. When we compare the inner and outer maltoside GTMs (GTM-Is *vs* GTM-Os), it is anticipated that the outer maltoside version (GTM-O) has a higher hydrophobic density than the inner maltoside version (GTM-I) due to the connections of the main alkyl chains into the *inner* hydroxyl groups of the glycerol unit. However, only little or small difference in detergent efficacy was observed between the regio-isomers of E/M-GTMs (E/M-GTM-O *vs* E/M-GTM-I), likely associated with the minor differences in their water solubility, CACs and aggregate sizes. Therefore, this analysis reveals that the variation in pendant polarity rather than the relative location of the detergent head and tail groups, by virtue of the significant change in GTM conformation, plays a dominant role in detergent efficacy for protein stabilization. A favorable effect of a detergent hydrophobic pendant on protein stability was previously reported [73], but there

is little study describing the favorable effect of a hydrophilic pendant on membrane protein stability. Furthermore, the dramatic change in detergent conformation resulting from pendant polarity variation is conceptually new and the detergent design principle obtained here would facilitate development of promising new detergents for membrane protein study.

There is still substantial possibility for further structural variations in GTM architecture. One simple variation is to introduce another head group such as a glucoside, oligoglycerol, or phophocholine into the GTM architecture as head group identity often dramatically changes detergent utility in diverse applications for membrane protein study [32,75]. Alternatively, it would be interesting to introduce versatile hydrophilic/hydrophobic pendants into the detergent core unit. Introduction of pendants with different sizes/volumes into the detergent hydrophilic-hydrophobic interfaces not only allows systematic modification of the detergent geometry, but also provides an effective means to vary the hydrophobic or hydrophilic density in detergent aggregates. Detergent geometry and hydrophobic density both are important in terms of self-assembly behavior and protein stabilization [38,79]. Finally, we can implant an additional function into detergent molecules by introducing a specifically functionalized pendant group. For example, fluorescent detergents could be prepared using fluorophores as the pendants, which allows us to tract detergent micelles and a target protein encapsulated by the detergent molecules for membrane protein manipulation. A GTM molecule with photo-active pendant can be prepared using a photo-responsive linker between the pendant and the detergent core unit. Recently, photo-cleavable detergents have found utility in membrane protein analysis via native mass spectrometry [76,77]. As GTM molecules are sufficiently large, structural variations in the pendant group should have little effect on the detergent efficacy for protein stabilization, but enrich the repertoire of this class of detergents for membrane protein research.

5. Conclusions

We synthesized the hydrophobic or hydrophilic pendant-bearing GTMs with the highly flexible core unit and explored the effects of the structural variations on detergent self-assemblies and membrane protein stability. The current study reveals that the hydrophilic pendant-bearing GTMs (M-GTMs), particularly M-GTM-O10, M-GTM-O11, and M-GTM-I11, were markedly superior to DDM and the hydrophobic ethyl pendant-bearing GTMs (E-GTMs) at stabilizing the tested membrane proteins here. In addition, M-GTM-O12 of the M-GTMs conferred notably marked stability to two GPCRs (human β_2AR and mouse MOR) compared to DDM and LMNG. The pendant polarity-directed detergent conformation and resulting high alkyl chain density in the self-assembly interiors are responsible for enhanced efficacy of the M-GTMs for protein stabilization. This study shows that detergent self-assemblies and membrane protein stability can be effectively controlled by detergent pendant polarity, with contributions of detergent alkyl chain length and the relative position of the head and tail groups.

Author disclosure statement

The authors declare the following competing financial interest(s): P.S.C., A.S. and H.E.B. are inventors on a patent application that covers the GTM agents.

Acknowledgements

This work was supported by LG Yonam Foundation of Korea. This work was also supported by the National Research Foundation of Korea (NRF) (2021R1A2C2006067 and 2018R1A6A1A03024231 to P.S.C.). This study was also supported by the National Science Foundation (grant MCB-1810695 to W.I.) and the National Institutes of Health (grants R01GM122759 and R21NS105863 to L.G.). S.K. and Y.U. were supported by an individual grant of Korea Institute for Advanced Study (CG080501) and the Research Clerkship Program of Nara Medical University, Japan, respectively.

Supplementary data

Supplementary data to this article can be found online at https://doi.Org/10.1016/j.actbio.2021.xx.xxx.

References

1 E. Wallin, H.G. Von, Genome-wide analysis of integral membrane proteins from eubacterial, archaean, and eukaryotic organisms, Protein Sci. 7 (1998) 1029–1038.

2 S.J. Singer, Some early history of membrane protein biology, Annu. Rev. Physiol. 66 (2004) 1–27.

3 R. Lappano, M. Maggiolini, G protein-coupled receptors: novel targets for drug discovery in cancer, Nat. Rev. Drug Discovery 10 (2011) 47–60.

4 C.R. Sanders, J.K. Myers, Disease-related misassembly of membrane proteins, Annu. Rev. Biophys. Biomol. Struct. 33 (2004) 25–51.

5 M.M. Dailey, C. Hait, P.A. Holt, J.M. Maguire, J.B. Meier, M.C. Miller, L. Petraccone, J.O. Trent, Structure-based drug design: from nucleic acid to membrane protein targets, Exp. Mol. Pathol. 86 (2009) 141–150.

6 https://www.wwpdb.org/

7 J. Deisenhofer, O. Epp, K. Miki, R. Huber, H. Michel, Structure of the protein subunits in the photosynthetic reaction centre of *Rhodopseudomonas viridis* at 3Å resolution, Nature 318 (1985) 618−624.

8 Z. Yang, C. Wang, Q. Zhou, J. An, E. Hildebrandt, L.A. Aleksandrov, J.C. Kappes, L.J. DeLucas, J.R. Riordan, I.L. Urbatsch, J.F. Hunt, C.G. Brouillette, Membrane protein stability can be compromised by detergent interactions with the extramembranous soluble domains, Protein Sci. 23 (2014), 769–789.

9 J.L. Parker, S. Newstead, Current trends in α-helical membrane protein crystallization: an update, Protein Sci. 21 (2012) 1358-1365.

10 M.J. Serrano-Vega, F. Magnani, Y. Shibata, C.J. Tate, Conformational thermostabilization of the β1-adrenergic receptor in a detergent-resistant form, Proc. Natl. Acad. Sci. U. S. A. 105 (2008) 877−882.

11 S. Ewstead, S. Ferrandon, S. Iwata, Rationalizing α-helical membrane protein crystallization, Protein Sci. 17 (2008) 466−472.

12 Q. Zhang, H. Tao, W.-X. Hong, New amphiphiles for membrane protein structural biology, Methods 55 (2011) 318–323.

13 Y. Alguel, J. Leung, S. Singh, R. Rana, L. Civiero, C. Alves, B. Byrne, New tools for membrane protein research, Curr. Protein Pept. Sci. 11 (2010) 156-165.

14 R. Ujwal, J.U. Bowie, Crystalizing membrane proteins using lipidic bicelles, Methods 55 (2011) 337–341.

15 I.G. Denisov, S.G. Sligar, Nano discs for structural and functional studies of membrane proteins, Nat. Struct. Mol. Biol. 23 (2016) 481-486.

16 P. Bazzacco, E.B. Denis, K.S. Sharma, L.J. Catoire, S. Mary, C.L. Bon, E. Point, J.-L. Banères, G. Durand, F. Zito, P. Pucci, J.-L. Popot, Trapping and Stabilization of Integral Membrane Proteins by Hydrophobically Grafted Glucose-Based Telomers, Biochemistry 51 (2012) 1416–1430.

17 J.M.Dörr, S. Scheidelaar, M.C. Koorengevel, J.J. Dominguez, M. Schäfer, C.A. Van Walree, J. A. Killian, The styrene–maleic acid copolymer: a versatile tool in membrane research, Eur. Biophys. J. 45 (2016) 3–21.

18 C.-L. McGregor, L. Chen, N.C. Pomroy, P. Hwang, S. Go, A. Chakrabartty, G.G. Privé, Lipopeptide detergents designed for the structural study of membrane proteins, Nat. Biotechnol. 21 (2003) 171-176.

19 J. Frauenfeld, R. Löving, J.P. Armache, A.F. Sonnen, F. Guettou, P. Moberg, L. Zhu, C. Jegerschöld, A. Flayhan, J.A. Briggs, H. Garoff, A saposin-lipoprotein nanoparticle system for membrane proteins, Nat. Methods 13 (2016) 345-351.

20 P.S. Chae, R.R. Rana, K. Gotfryd, S.G.F. Rasmussen, A.C. Kruse, K.H. Cho, S. Capaldi, E. Carlsso, B. Kobilka, C.J. Loland, U. Gether, S. Banerjee, B. Byrne, J.K. Lee, S.H. Gellman, Glucose-neopentyl glycol (GNG) amphiphiles for membrane protein study, Chem. Commun. 49 (2013) 2287–2289.

21 P.S. Chae, S.G.F. Rasmussen, R.R. Rana, K. Gotfryd, R. Chandra, M.A. Goren, A.C. Kruse, S. Nurva, C.J. Loland, Y. Pierre, D. Drew, J.L. Popot, D. Picot, B.G. Fox, L. Guan, U. Gether, B. Byrne, B. Kobilka, S.H. Gellman, Maltose–neopentyl glycol (MNG) amphiphiles for solubilization, stabilization and crystallization of membrane proteins, Nat. Methods 7 (2010) 1003–1008.

22 A. Sadaf, J.S. Mortensen, S. Capaldi, E. Tikhonova, P. Hariharan, O. Ribeiro, C.J. Loland, L. Guan, B. Byrne, P.S. Chae, A class of rigid linker-bearing glucosides for membrane protein structural study, Chem. Sci. 7 (2016) 1933–1939.

23 S.C. Howell, R. Mittal, L. Huang, B. Travis, R.M. Breyer, C.R. Sanders, N.J. Fraser, CHOBIMALT: a cholesterol-based detergent, Biochemistry 49 (2010) 9572-9583.

24 P.S. Chae, S.G.F. Rasmussen, R.R. Rana, K. Gotfryd, A.C. Kruse, A. Manglik, K.H. Cho, S. Nurva, U. Gether, L. Guan, C.J. Loland, B. Byrne, B.K. Kobilka, S.H. Gellman, A New Class of Amphiphiles Bearing Rigid Hydrophobic Groups for Solubilization and Stabilization of Membrane Proteins, Chem.-Eur. J. 18 (2012) 9485–9490.

25 M. Das, Y. Du, J.S. Mortensen, H.E. Bae, B. Byrne, C.J. Loland, B.K. Kobilka, P.S. Chae, An Engineered Lithocholate-Based Facial Amphiphile Stabilizes Membrane Proteins: Assessing the Impact of Detergent Customizability on Protein Stability, Chem. Eur. J. 24 (2018) 9860-9868.

26 M. Ehsan, Y. Du, J.S. Mortensen, P. Hariharan, Q. Qu, L. Ghani, M. Das, A. Grethen, B. Byrne, G. Skiniotis, S. Keller, C.J. Loland, L. Guan, B.K. Kobilka, P.S. Chae, Self-Assembly Behavior and Application of Terphenyl-Cored Trimaltosides for Membrane-Protein Studies: Impact of Detergent Hydrophobic Group Geometry on Protein Stability, Chem. Eur. J. 25 (2019) 11545-11554.

27 M. Ehsan, Y. Du, N.J. Scull, E. Tikhonova, J. Tarrasch, J.S. Mortensen, C.J. Loland, G. Skiniotis, L. Guan, B. Byrne, B.K. Kobilka, P.S. Chae, Highly branched pentasaccharide-bearing amphiphiles for membrane protein studies, J. Am. Chem. Soc. 138 (2016) 3789−3796.

28 L.H. Urner, I. Liko, H.Y. Yen, K.-K. Hoi, J.R. Bolla, J. Gault, F.G. Almeida, M.-P. Schweder, D. Shutin, S. Ehrmann, R. Haag, C.V. Robinson, K. Pagel, Modular detergents tailor the purification and structural analysis of membrane proteins including G-protein coupled receptors, Nat. Commun. 11 (2020) 1-10.

29 A. Polidori, S. Raynal, L.-A. Barret, M. Dahani, C. Barrot-Ivolot, C. Jungas, E. Frotscher, S. Keller, C. Ebel, C. Breyton, F. Bonneté, Sparingly fluorinated maltoside-based surfactants for membrane-protein stabilization, New J. Chem. 40 (2016) 5364-5378.

30 A. Sadaf, Y. Du, C. Santillan, J.S. Mortensen, I. Molist, A.B. Seven, P. Hariharan, G. Skiniotis, C.J. Loland, B.K. Kobilka, L. Guan, B. Byrne, P.S. Chae, Dendronic trimaltose amphiphiles (DTMs) for membrane protein study, Chem. Sci. 8 (2017) 8315−8324.

31 D.M. Rosenbaum, C. Zhang, J. Lyons, R. Holl, D. Aragao, D.H. Arlow, S.G.F. Rasmussen, H.-J.Choi, B.T. DeVree, R.K. Sunahara, P.S. Chae, S.H. Gellman, R.O. Dror, D.E. Shaw, W.I. Weis, M. Caffrey, P. Gmeiner, B.K. Kobilka, Structure and Function of an Irreversible Agonist-β2 Adrenoceptor Complex, Nature 469 (2011) 236–240.

32 A.M. Ring, A. Manglik, A.C. Kruse, M.D. Enos, W.I. Weis, K.C. Garcia, B.K. Kobilka, Adrenaline-activated structure of β2-adrenoceptor stabilized by an engineered nanobody, Nature 502 (2013) 575–579.

33 H. Guo, S.A. Bueler, J.L. Rubinstein, Atomic model for the dimeric F_O region of mitochondrial ATP synthase, Science 358 (2017) 936-940.

34 A. Sadaf, M. Ramos, J.S. Mortensen, Y. Du, H.E. Bae, C.F. Munk, P. Hariharan, B. Byrne, B.K. Kobilka, C.J. Loland, L. Guan, P.S. Chae, Conformationally restricted monosaccharide-cored glycoside amphiphiles: the effect of detergent head group variation on membrane protein stability, ACS Chem. Biol. 14 (2019) 1717-1726.

35 M. Das, Y. Du, J.S. Mortensen, M. Ramos, L. Ghani, H.J. Lee, H.E. Bae, B. Byrne, L. Guan, C.J. Loland, B.K. Kobilka, P.S. Chae, Trehalose-cored amphiphiles for membrane protein stabilization: importance of the detergent micelle size in GPCR stability, Org. Biomol. Chem. 17 (2019) 3249−3257.

36 H. Hussain, Y. Du, E. Tikhonova, J.S. Mortensen, O. Ribeiro, C. Santillan, M. Das, M. Ehsan, C.J. Loland, L. Guan, B.K. Kobilka, B. Byrne, P.S. Chae, Resorcinarene-based glycosides for membrane protein study, Chem.-Eur. J. 23 (2017) 6724-6729.

37 R.M. Merheb, M. Rhimi, A. Leydier, F. Huché, C. Galián, E.D. Mandon, D. Ficheux, D. Flot, N. Aghajari, R. Kahn, A.D. Pietro, J.-M. Jault, A.W. Coleman, P. Falson, Structuring Detergents for Extracting and Stabilizing Functional Membrane Proteins, PLoS One 6 (2011) e18036.

38 M. Das, Y. Du, O. Ribeiro, P. Hariharan, J.S. Mortensen, D. Patra, G. Skiniotis, C.J. Loland, L. Guan, B.K. Kobilka, B. Byrne, P.S. Chae, Conformationally preorganized diastereomeric norbornane-based maltosides for membrane protein study: Implications of detergent kink for micellar properties, J. Am. Chem. Soc. 139 (2017) 3072−3081.

39 L. Ghani, C.F. Munk, X. Zhang, S. Katsube, Y. Du, C. Cecchetti, W. Huang, H.E. Bae, S. Saouros, M. Ehsan, L. Guan, X. Liu, C.J. Loland, B.K. Kobilka, B. Byrne, P.S. Chae, 1,3,5-Triazine-Cored Maltoside Amphiphiles for Membrane Protein Extraction and Stabilization, J. Am. Chem. Soc., 141 (2019) 19677-19687.

40 S. Jo, T. Kim, V.G. Iyer, W. Im, CHARMM-GUI: a web-based graphical user interface for CHARMM, J. Comput. Chem. 29 (2008) 1859-1865.

41 X. Cheng, S. Jo, H.S. Lee, J.B. Klauda, W. Im, CHARMM-GUI micelle builder for pure/mixed micelle and protein/micelle complex systems, J. Chem. Inf. Model 53 (2013) 2171-2180.

42 E.L. Wu, X. Cheng, S. Jo, H. Rui, K.C. Song, E.M. Davila-Contreras, Y.F. Qi, J.M. Lee, V. Monje-Galvan, R.M.Venable, J.B. Klauda, W. Im, CHARMM-GUI Membrane Builder Toward Realistic Biological Membrane Simulations, J. Comput. Chem. 35 (2014) 1997-2004.

43 J.B. Klauda, R.M. Venable, J.A. Freites, J.W.O'Connor, D.J. Tobias, C. Mondragon-Ramirez, I. Vorobyov, A.D. Jr. MacKerell, R.W. Pastor, Update of the CHARMM all-atom additive force field for lipids: validation on six lipid types, J. Phys. Chem. B 114 (2010) 7830-7843.

44 O. Guvench, E. Hatcher, R.M. Venable, R.W. Pastor, A.D. MacKerell, CHARMM Additive All-Atom Force Field for Glycosidic Linkages between Hexopyranoses, J. Chem. Theory Comput. 5 (2009) 2353-2370.

45 O. Uvench, S.S. allajosyula, E.P. Raman, E. Hatcher, K. Vanommeslaeghe, T.J. Foster, F.W. Jamison, A.D. MacKerell, J. Chem. Theory Comput. 7 (2011) 3162-3180.

46 A.N. Leonard, R.W. Pastor, J.B. Klauda, Parameterization of the CHARMM All-Atom Force Field for Ether Lipids and Model Linear Ethers, J. Phys. Chem. B 122 (2018) 6744-6754.

47 W.L. Jorgensen, J. Chandrasekhar, J.D. Madura, R.W. Impey, M.L. Klein, Comparison of Simple Potential Functions for Simulating Liquid Water, J. Phys. Chem. 79 (1983) 926-935.

48 P. Eastman, J. Swails, J.D. Chodera, R.T. McGibbon, Y.T. Zhao, K.A. Beauchamp, L.P. Wang, A.C. Simmonett, M.P. Harrigan, C.D. Stern, R.P. Wiewiora, B.R. Brooks, V.S. Pande, OpenMM 7: Rapid development of high performance algorithms for molecular dynamics, Plos Comput. Biol. 13 (2017) e100565910.

49 J. Lee, X. Cheng, J.M. Swails, M.S. Yeom, P.K. Eastman, J.A. Lemkul, S. Wei, J. Buckner, J.C. Jeong, Y.F. Qi, S. Jo, V.S. Pande, D.A. Case, C.L. Brooks, A.D. MacKerell, J.B. Klauda, W. Im, CHARMM-GUI Input Generator for NAMD, GROMACS, AMBER, OpenMM, and CHARMM/OpenMM Simulations Using the CHARMM36 Additive Force Field, J. Chem. Theory Comput. 12 (2016) 405-413.

50 C.B. Billesbølle, M.B. Kruger, L. Shi, M. Quick, Z. Li, S. Stolzenberg, J. Kniazeff, K. Gotfryd, J.S. Mortensen, J.A. Javitch, H. Weinstein, C.J. Loland, U. Gether, Substrate-induced unlocking of the inner gate determines the catalytic efficiency of a neurotransmitter:sodium symporter, J. Biol. Chem. 44 (2015) 26725-26738.

51 M. Quick, J.A. Javitch, Monitoring the function of membrane transport proteins in detergent-solubilized form, Proc. Natl. Acad. Sci. U. S. A. 9 (2007) 3603-3608.

52 H.R. Kaback, Methods Enzymol. 22 (1971) 99-120.

53 S.A. Short, H.R. Kaback, L.D. Kohn, D-lactate dehydrogenase binding in *Escherichia coli* dld$^-$ membrane vesicles reconstituted for active transport, Proc. Natl. Acad. Sci. U. S. A. 71 (1974) 1461-1465.

54 L. Guan, S. Nurva, S.P. Ankeshwarapu, Mechanism of melibiose/cation symport of the melibiose permease of *Salmonella typhimurium*. J. Biol. Chem. 286 (2011) 6367−6374.

55 A.S. Ethayathulla, M.S. Yousef, A. Amin, G. Leblanc, H.R. Kaback, L. Guan, Structure-based mechanism for Na+/melibiose symport by MelB, Nat. Commun. 5 (2014) 3009.

56 E. Cordat, I. Mus-Veteau, G. Leblanc, Structural Studies of the Melibiose Permease of *Escherichia coli* by Fluorescence Resonance Energy Transfer II. Identification of the tryptophan residues acting as energy donors, J. Biol. Chem. 273 (1998) 33198−33202.

57 D.M. Rosenbaum, V. Cherezov, M.A. Hanson, S.G.F. Rasmussen, F.S. Thian, T.S. Kobilka, H.J. Choi, X.J. Yao, W.I. Weis, R.C. Stevens, B.K. Bobilka, GPCR engineering yields high-resolution structural insights into β2-adrenergic receptor function, Science 318 (2007) 1266–1273.

58 B.K. Kobilka, Amino and carboxyl terminal modifications to facilitate the production and purification of a G protein-coupled receptor, Anal. Biochem. 231 (1995) 269–271.
59 A. Koehl, H. Hu, S. Maeda, Y. Zhang, Q. Qu, J.M. Paggi, N.R. Latorraca, D. Hilger, R. Dawson, H. Matile, G.F.X. Schertler, S. Granier, W.I. Weis, R.O. Dror, A. Manglik, G. Skiniotis, B.K. Kobilka, Structure of the μ-opioid receptor-Gi protein complex, Nature 558 (2018) 547–552.
60 B.W. Berger, R.Y. García, A.M. Lenhoff, E.W. Kaler, C.R. Robinson, Relating surfactant properties to activity and solubilization of the human adenosine A_3 receptor, Biophys J. 89 (2005) 452–464.
61 K.H. Cho, P. Hariharan, J.S. Mortensen, Y. Du, A. Nielsen, B. Byrne, B.K. Kobilka, C.J. Loland, L. Guan, P.S. Chae, Isomeric Detergent Comparison for Membrane Protein Stability: Importance of Inter-Alkyl-Chain Distance and Alkyl Chain Length, ChemBioChem 17 (2016) 2334−2339.
62 J. Israelachvili, D.J. Mitchell, B.W. Ninham, Theory of self-assembly of hydrocarbon amphiphiles into micelles and bilayers, J. Chem. Soc. Faraday Trans. 2 (1976) 1525-1568.
63 R.C. Oliver, J. Lipfert, D.A. Fox, R.H. Lo, S. Doniach, L. Columbus, Dependence of Micelle Size and Shape on Detergent Alkyl Chain Length and Head Group, PLoS ONE 8 (2013) 1-10.
64 A. Chattopadhyay, E. London, Fluorimetric determination of critical micelle concentration avoiding interference from detergent charge, Anal. Biochem. 139 (1984) 408−412.
65 G. Deckert, P.V. Warren, T. Gaasterland, W.G. Young, A.L. Lenox, D.E. Graham, R. Overbeek, M.A. Snead, M. Keller, M. Aujay, R. Huber, R.A. Feldman, J.M. Short, G.J. Olsen, R.V. Swanson, The complete genome of the hyperthermophilic bacterium *Aquifex aeolicus*, Nature 392 (1998) 353–358.
66 H.E. Hart, E.B. Greenwald, Scintillation proximity assay (SPA)-a new method of immunoassay. Direct and inhibition mode detection with human albumin and rabbit antihuman albumin, Mol. Immunol. 16 (1979) 265-267.
67 P. Hariharan, L. Guan, Thermodynamic cooperativity of co-substrate binding and cation selectivity of *Salmonella typhimurium* MelB, J. Gen. Physiol. 149 (2017) 1029–1039.
68 C. Maehrel, E. Cordat, I. Mus-Veteau, G. Leblanc, Structural Studies of the Melibiose Permease of *Escherichia coli* by Fluorescence Resonance Energy Transfer, J. Biol. Chem. 273 (1998) 33192-33197.
69 A. Amin, P. Hariharan, P.S. Chae, L. Guan, Effect of detergents on galactoside binding by Melibiose permeases, Biochemistry 54 (2015) 5849−5855.
70 X. Yao, C. Parnot, X. Deupi, V.R. Ratnala, G. Swaminath, D. Farrens, B. Kobilka, Coupling ligand structure to specific conformational switches in the β2-adrenoceptor, Nat. Chem. Biol. 2 (2006) 417−422.
71 A. Manglik, A.C. Kruse, T.S. Kobilka, F.S. Thian, J.M. Mathiesen, R.K. Sunahara, L. Pardo, W.I. Weis, B.K. Kobilka, S. Granier, Crystal structure of the μ-opioid receptor bound to a morphinan antagonist, Nature 485 (2012) 321-326.
72 A.W.R. Serohijos, S. Yin, F. Ding, J. Gauthier, D.G. Gibson, W. Maixner, N.V. Dokholyan, L. Diatchenko, Structural basis for μ-opioid receptor binding and activation, Structure 19 (2011) 1683-1690.
73 H.E. Bae, C. Cecchetti, Y. Du, S. Katsube, J.S. Mortensen, W. Huang, S. Rehan, H.J. Lee, C.J. Loland, L. Guan, B.K. Kobilka, B. Byrne, P.S. Chae, Pendant-bearing glucose-neopentyl glycol

(P-GNG) amphiphiles for membrane protein manipulation: Importance of detergent pendant chain for protein stabilization, Acta Biomaterialia 112 (2020) 250-261.
74 G.G. Privé, Detergents for the stabilization and crystalization of membrane proteins, Methods 41 (2007) 388-397.
75 J. Breibeck, A. Rompel, Successful amphiphiles as the key to crystallization of membrane proteins: Bridging theory and practice, Biochim. Biophys. Acta. 1863 (2019) 437-455.
76 N.P. Barrera, C.V. Robinson, Advances in the mass spectrometry of membrane proteins: From individual proteins into intact complexes, Annu. Rev. Biochem. 80 (2011) 247-271.
77 K.A. Brown, B. Chen, T.M. Guardado-Alvarez, Z. Lin, L. Hwang, S. Ayaz-Guner, S. Jin, Y. Ge, A photocleavable surfactant for top-down proteomics, Nat. Methods 16 (2019) 417-420.

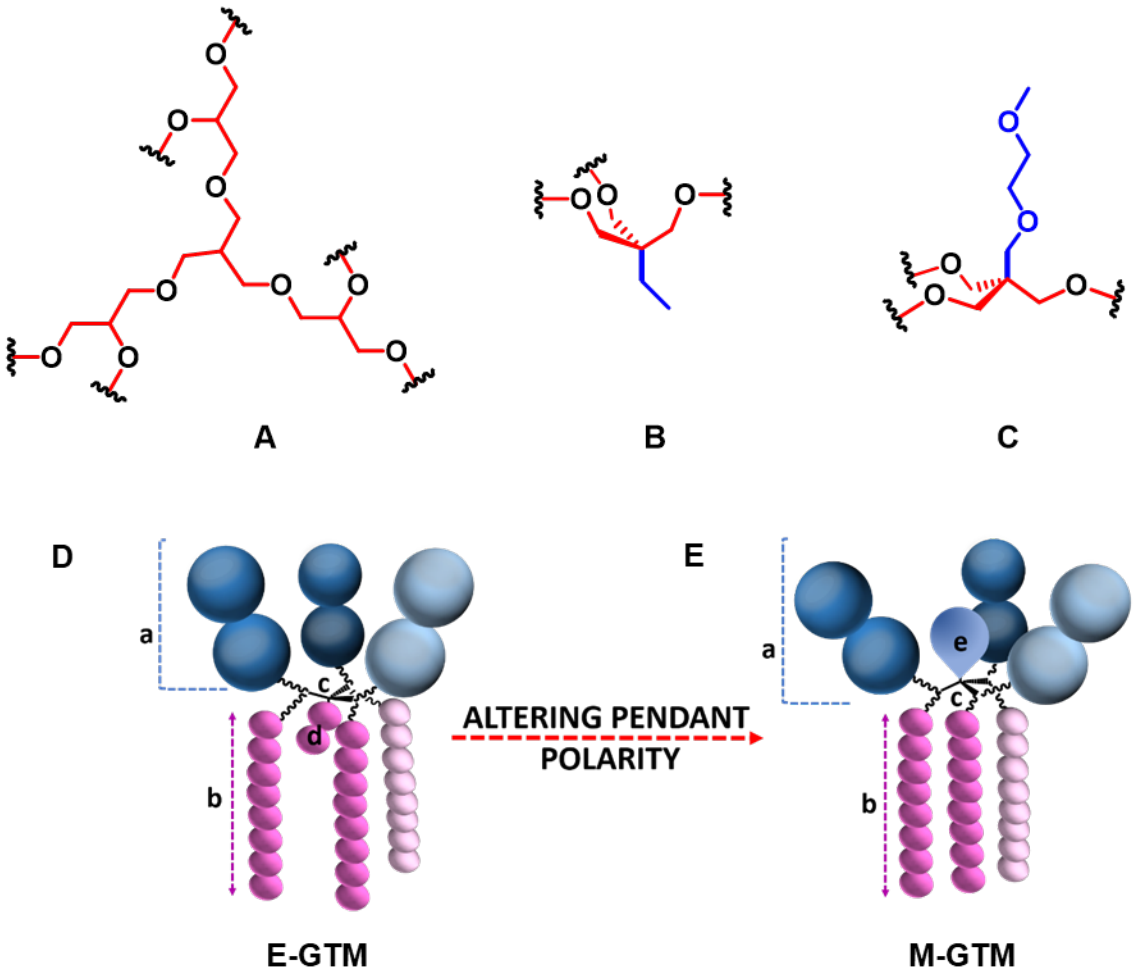

Figure 1 Detergent design and conformations. (A) Top view of the glycerol-decorated tris(hydroxymethyl)methane (THM) core unit used for preparation of E/M-GTMs. The fourth substituent (i.e., pendant chain) attached into the central carbon was omitted for clarity. (B,C) Side view of the central THM unit of E/M-GTMs indicating the direction of the pendant chain (ethyl or methoxyethoxylmethyl (MEM)) depending on their hydrophobicity/hydrophilicity in aqueous solution. Note the opposite directions of the pendant chains and the central carbons of the THM units, resulting in a large variation in the conformation of the detergent core unit. The pendant chains of E-GTMs and M-GTMs are indicated in blue. (D,E) Schematic representations of E-GTM (D) and M-GTM conformation (E) under micellar conditions. The presence of the pendant chains with an opposite polarity in the hydrophobic-hydrophilic interfaces leads to a different molecular conformation in the central region between the E-GTMs and M-GTMs. This results in the large hydrophobic and hydrophilic volumes for the E- and M-GTMs, respectively. a: Maltoside head groups; b: Main alkyl chains; c: Glycerol-decorated THM core; d: Ethyl pendant; e: MEM pendant.

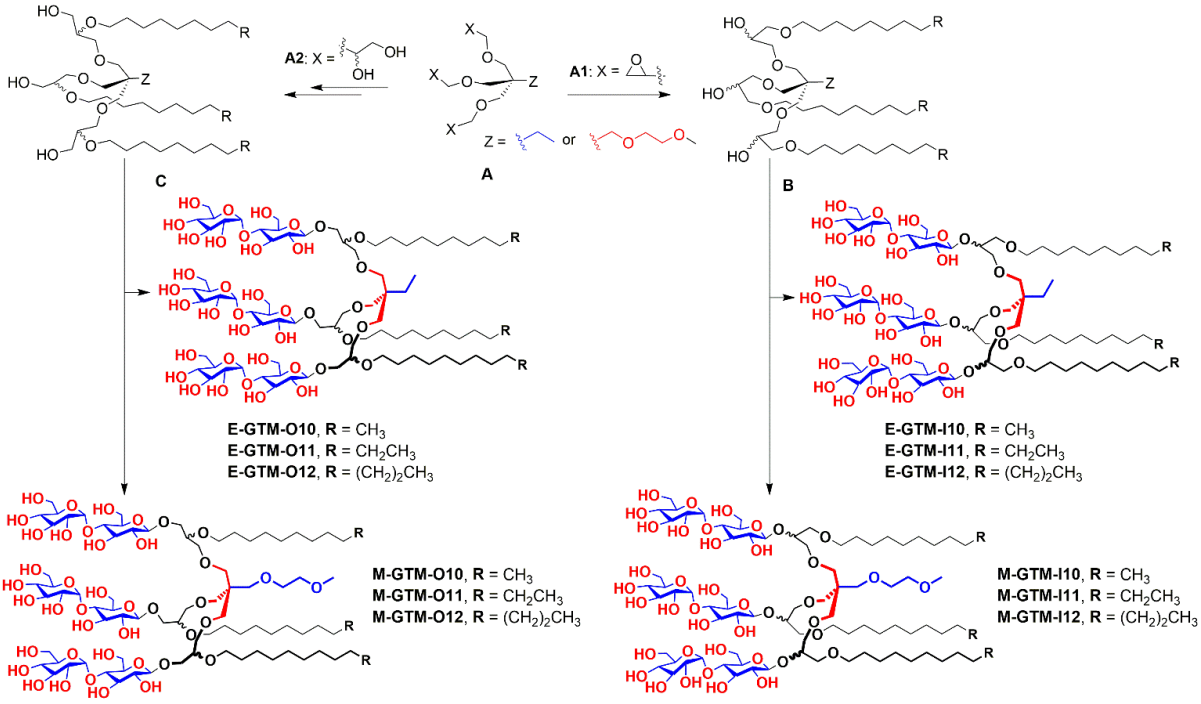

Scheme 1 Detergent synthetic scheme. Ethyl or MEM pendant-bearing triglycidal ether derivative (**A1**) was used as a starting material for preparation of the inner maltoside versions (E/M-GTM-Is), while the outer maltoside versions (E/M-GTM-Os) were prepared from a glycerol-decorated THM derivative with an ethyl or MEM chain (**A2**). A regio-selective epoxide ring opening of **A1** with an alkoxide yielded the triol derivatives (**B**) with the three alkyl chains attached to the *outer* hydroxyl groups (1°) via ether linkages. The selective introduction of the three alkyl chains into the secondary hydroxyl groups (2°) of **A2** utilizing TBDMS protection led to preparation of the triol derivatives (**C**) with the three alkyl chains attached to the *inner* hydroxyl groups (1°). Glycosylation of the resulting triol derivatives (**B** and **C**), followed by a global deprotection, provided the inner and outer maltoside amphiphiles (E/M-GTM-Is and E/M-GTM-Os, respectively). The presence of stereo-chemically ill-defined carbons is indicated in wavy lines in the chemical structures.

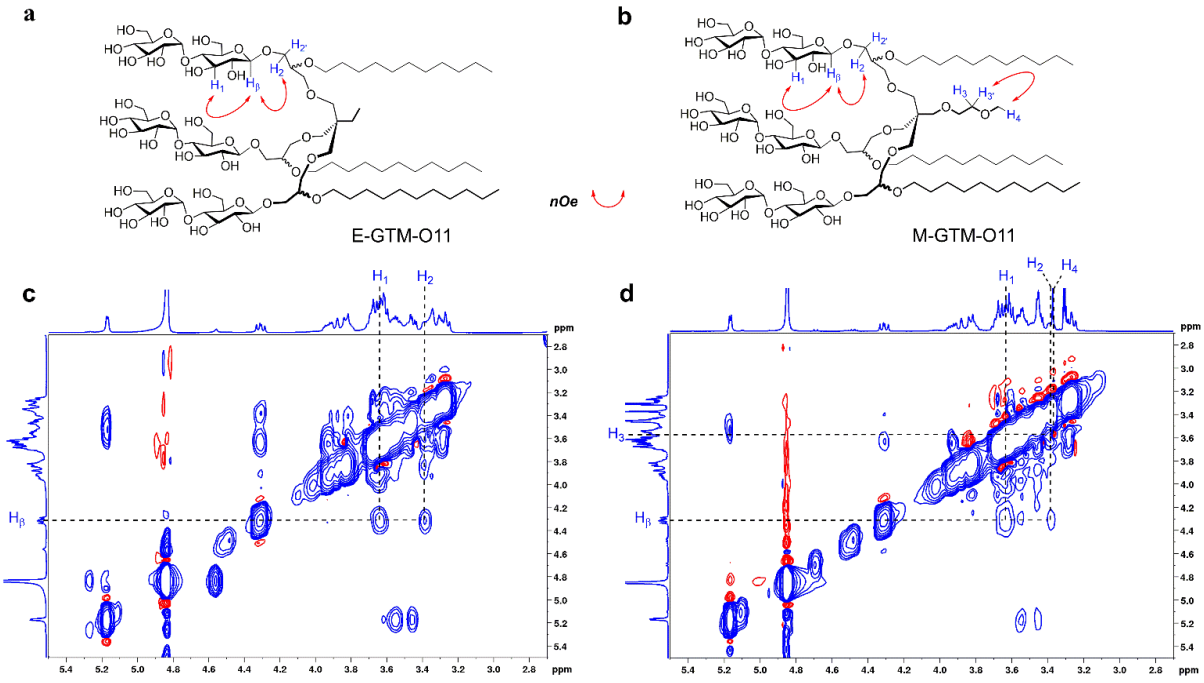

Figure 2 Partial 2D NOESY spectra of E-GTM-O11 and M-GTM-O11. (a,b) Chemical structures of E-GTM-O11 and M-GTM-O11 were inserted to indicate a few sets of protons displaying main NOE correlations in the spectra. (c,d) A strong NOE correlation signal was found between the β-anomeric proton (H_β) and the C3-axial proton (H_1), supporting β-glycosidic bond formation in both detergents. The strong correlation of the β-anomeric proton to the glycerol proton (H_2) reflects the connectivity between the maltose head group and the glycerol linker. In the case of M-GTM-O11, a correlation between two pendant protons (H_3 and H_4) was detected. These through-space interactions were represented by red arrows in the chemical structures of E-GTM-O11 and M-GTM-O11 (a,b) and the associated correlation signals were indicated by the dotted lines in their NOESY spectra (c,d). Further analysis for NOE correlation signals and their assignments were found in Figure S4.

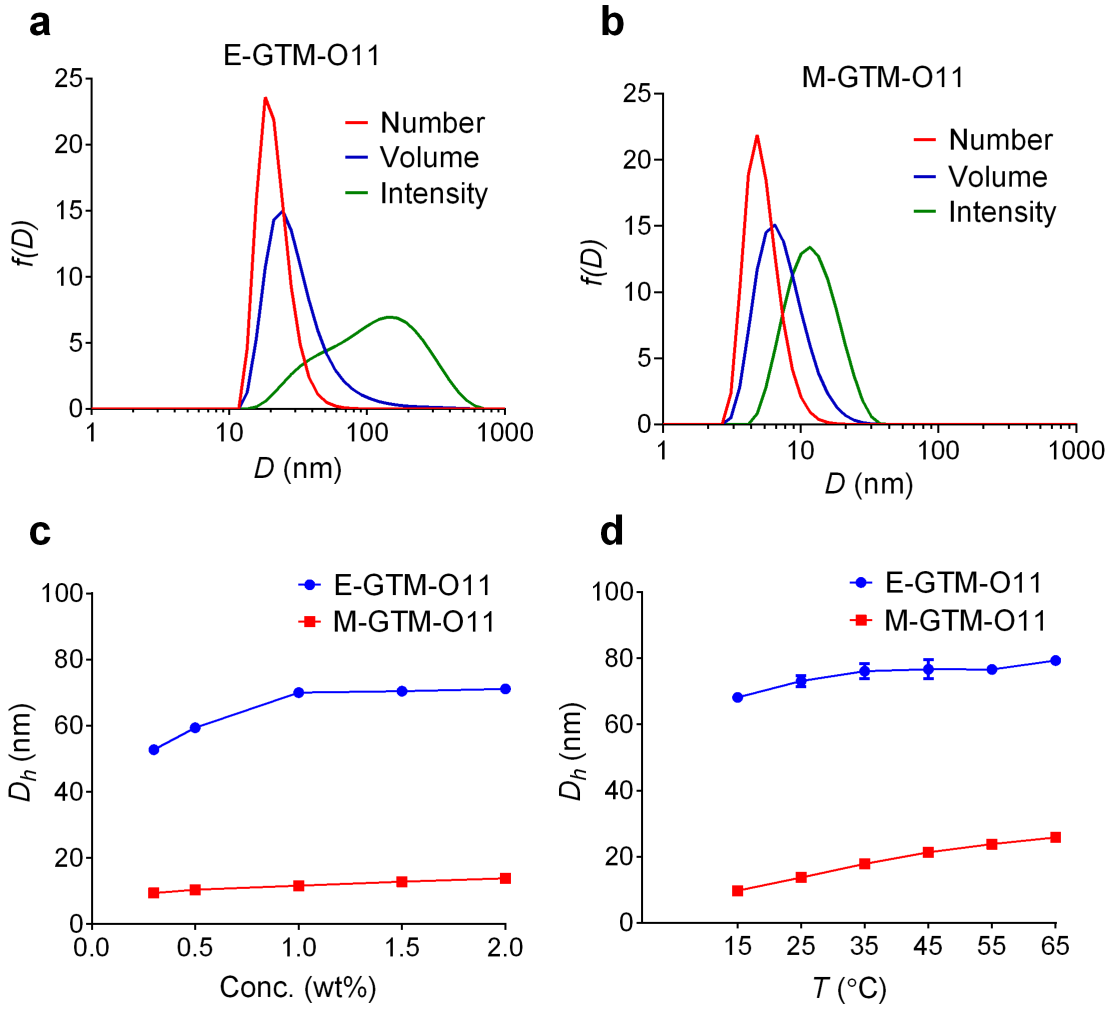

Figure 3 Detergent DLS profiles. Number, volume, and intensity-weighted DLS profiles of E-GTM-O11 (a) and M-GTM-O11 (b), and the size variation in self-assemblies formed by these detergents depending on detergent concentration (c) and solution temperature (d). (a,b) The DLS profiles were measured at 25 °C using 1.0 wt% detergent concentration. (c,d) Self-assembly sizes (D_h) of the detergents were measured in a range of detergent concentrations from 0.3 to 2.0 wt% (c), or monitored with a variation of solution temperature from 15 to 65 °C (d). Solution temperature was kept at 25 °C during detergent concentration variation, while detergent concentration was maintained at 1.0 wt% over the course of solution temperature variation.

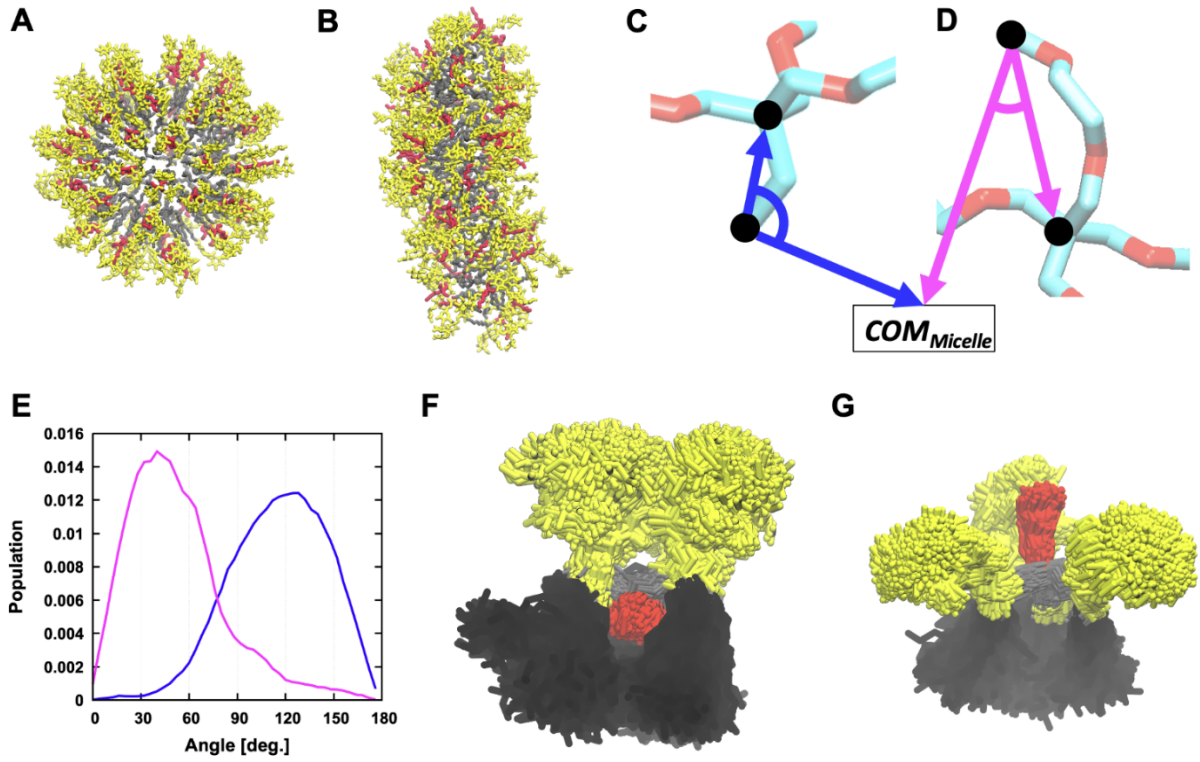

Figure 4 MD simulation results of detergent aggregates. (A,B) Initial structure and lateral view of M-GTM-O10 aggregates at 400 ns (water and ions not shown for clarity): yellow sticks for maltoses, gray sticks for alkyl chains and red sticks for pendants, respectively. (C-E) Pendant direction indicated by angles between three points; the center of mass (COM) of the aggregates, the center carbon of the THM core unit, and the last carbon of the pendant in (C) E-GTM-O10 and (D) M-GTM-O10, and (E) resulting three-point angle distribution for each pendant during MD simulations: E-GTM-O10 (blue) and M-GTM-O10 (magenta). (F,G) Side views of overlaid snapshot in the last 100-ns simulation for (F) E-GTM-O10 and (G) M-GTM-O10 monomers each located at the center of bicelle-like detergent aggregates.

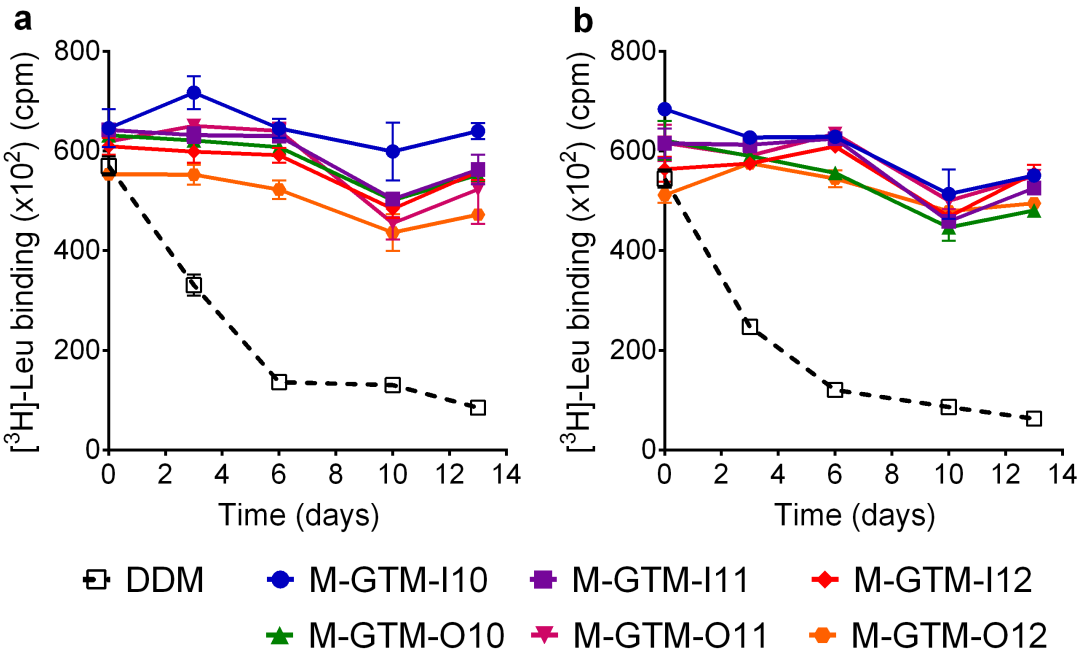

Figure 5 Time-course stability of LeuT. The detergents were tested at CMCs + 0.04 (a) or 0.2 wt% (b). DDM-purified LeuT was diluted into buffer solutions containing the individual M-GTMs or DDM. The resulting sample solutions were incubated for 13 days at room temperature. The ability of the transporter to bind the radio-active substrate ([^{3}H]-leucine (Leu)) was measured at regular intervals during the incubation using scintillation proximity assay (SPA). Data are shown as means ± SEM (error bars), *n* = 3.

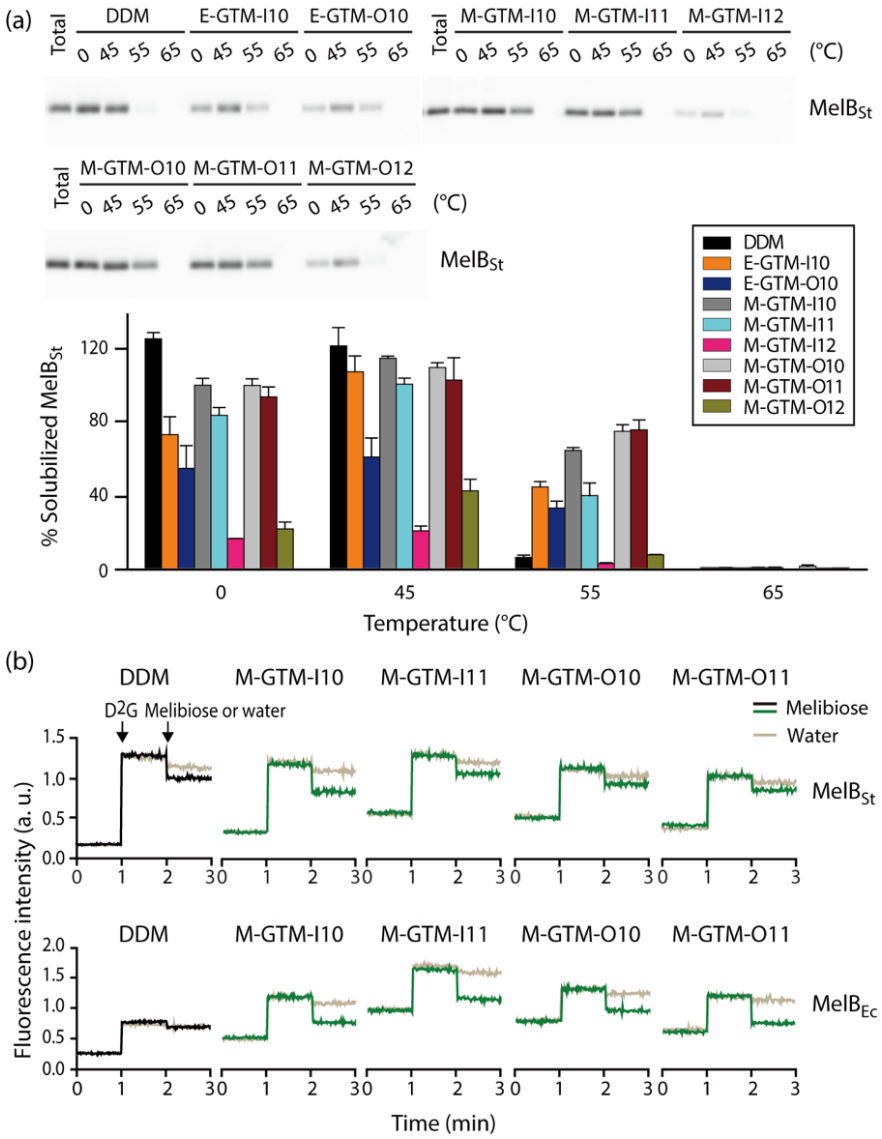

Figure 6 Temperature-dependent $MelB_{St}$ solubility. *E. coli* membranes containing $MelB_{St}$ were treated with 1.5 wt% individual detergents for 90 min at 0 °C. The detergent-extracted samples were further incubated at an elevated temperature (45, 55, or 65 °C) for another 90 min. Soluble fractions were isolated from the sample solutions *via* ultracentrifugation. The amount of soluble $MelB_{St}$ in each condition was analyzed by SDS-PAGE and Western blot (*top*) and the data obtained is summarized in the histogram (*bottom*). The initial amount of soluble $MelB_{St}$ in the untreated membranes was used a reference (100%), designated 'Total' in (a). Error bars, SEM, n = 2-3. (b) MelB functional analysis *via* a galactoside binding assay. Right-side-out (RSO) membrane vesicles containing $MelB_{St}$ or $MelB_{Ec}$ were treated with the four selected M-GTMs (M-GTM-I10/I11/O10/O11) and DDM at 1.0 wt% for 90 min at 0 °C. Changes in fluorescence intensity of the detergent-extracted MelB were monitored over the additions of D^2G (1-min) and melibiose (2-min) (black (DDM) or green lines (a new detergent)). For control data, water instead of melibiose was added (pale gold lines).

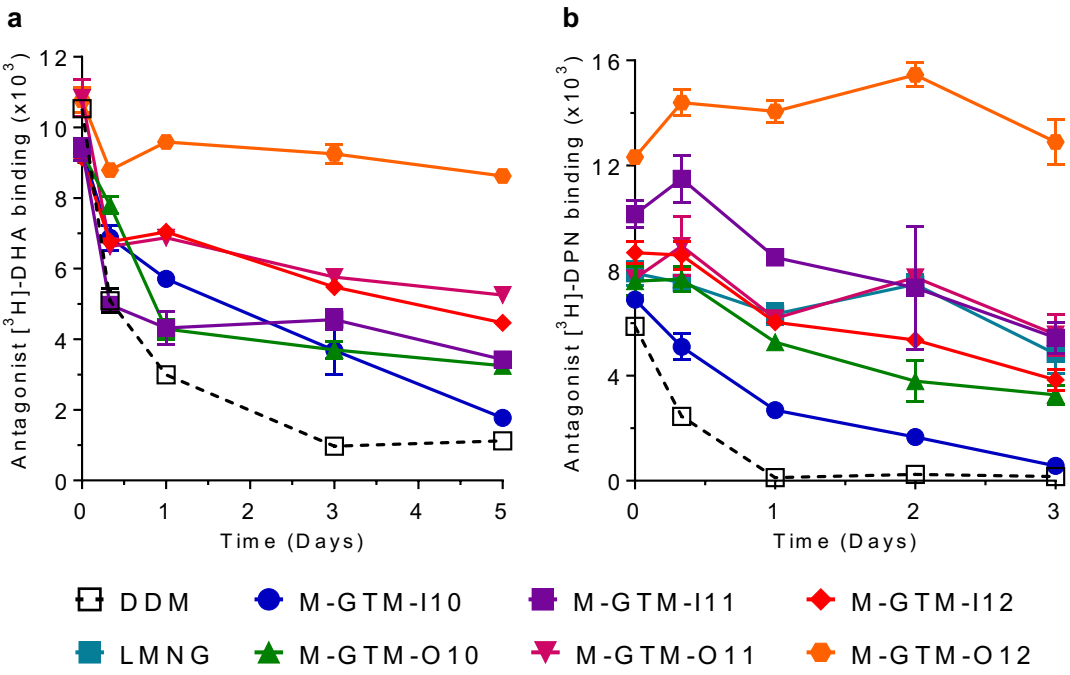

Figure 7 Long-term stability of two GPCRs (β_2AR and MOR) solubilized in the M-GTMs. DDM/LMNG was used as a control. DDM-purified β_2AR (a) and MOR (b) were diluted into buffer solutions including the individual detergents to give final detergent concentrations of 0.2 and 0.1 wt%, respectively. β_2AR and MOR stability was assessed by measuring the ability of the receptors to bind the radiolabeled ligand ([^{3}H]-dihydroalprenolol (DHA) and [^{3}H]-diprenorphine (DPN), respectively) at regular intervals during a 5 or 3-day incubation at room temperature. Data are shown as means ± SEM (error bars), *n* = 3.